ISOGEOMETRIC COLLOCATION METHOD FOR ELASTICITY PROBLEMS CONTAINING SINGULARITIES

by

Puja Rattan

A dissertation proposal submitted to the faculty of
The University of North Carolina at Charlotte
in partial fulfillment of the requirements
for the degree of Doctor of Philosophy in
Applied Mathematics

Charlotte

2016

Approved by:

_____

Dr. Hae-Soo Oh

_____

Dr. Shaozhong Deng

_____

Dr. Wei Cai

_____

Dr. Russell Keanini

ABSTRACT

PUJA RATTAN. Isogeometric collocation method for elasticity problems containing singularities. (Under the direction of DR. HAE-SOO OH)

Isogeometric analysis (IGA), introduced by Hughes, et al. [2,3], is a mathematical approach that combines Finite Element analysis (FEA) in conjunction with engineering design tools, such as CAD, which allows analysis, testing and redesign of structural elements via the same data set. Prior to implementing a new material into a manufacturing process, it is necessary to design the shape of the object and then analyze the durability of the design. Generally NURBS basis functions are used to design complex structures. Isogeometric analysis is effective in the design-analysis-manufacture loop.

Babuŝka and Oh [10] introduced mapping techniques called the Method of Auxiliary Mapping (MAM) to handle singularities that occur in partial differential equations (PDEs). However, this method is unable to follow the framework of IGA. Thus, we are looking for another way to handle singularity in IGA using the Collocation method.

In order to develop methodology for solving PDEs containing singularities, the B-spline basis functions are first modified using partition unity functions. By using these modified basis functions the neighborhood of singularity will be enriched so that they can capture the singular behavior of the true solution. In this dissertation, this method is tested to one-dimensional and two-dimensional problems. Also, this method is more effective and economical than other existing methods in han-

dling problems containing singularities because the Collocation method requires less computation than the Galerkin method or any other existing methods.

Schwarz alternating method in the framework of IGA-Collocation is also introduced in this dissertation. In this method, a domain is decomposed into two subdomains and then the problem is solved by solving subproblems in each subdomain. The iterative process starts with an initial guess and iterates until it arrives at a solution of desired accuracy. This technique has been applied to one- and two-dimensional problems for overlapping as well as non-overlapping subdomains. Elasticity problems containing singularities are also solved using this method. Numerical results are presented and compared with the results obtained by the IGA-Galerkin method.

DEDICATION

This thesis is dedicated to my loving family and to my parents for their endless love, support, encouragement and sacrifices.

ACKNOWLEDGMENTS

I would like to express my deep appreciation and gratitude to my advisor, Dr. Hae-Soo Oh, for the effective guidance and mentor-ship he has provided to me continuously. He is always very supportive and patient.

I would also like to thank the committee members, Drs. Shaozhong Deng and Wei Cai for their friendly guidance and thought provoking suggestions. I would like to thank Dr. Russell Keanini for agreeing to serve on my doctoral dissertation committee as an outside department committee member.

I would also like to thank Graduate School and Mathematics department for providing me financial support. Special thanks to Dr. Hyunju Kim who has helped me with computations at the beginning stage of my research. It would have been very difficult for me to compute numerical results if he had not helped me with the programming.

I would also like to thank my parents who have always been there for me, and came all the way from India to take care of my newborn daughter during the final stage of my PhD program. Without their blessings and support it would have been very difficult for me to achieve this dream.

Last but not the least I would like to thank my husband for the love, support, and constant encouragement he has given over the years. I undoubtedly could not have done this without his support and motivation. Finally, I would like to thank and dedicate this thesis to my daughter, Nyra who has been the most wonderful daughter anyone can have.

TABLE OF CONTENTS

LIST OF FIGURES

LIST OF TABLES

CHAPTER 1: INTRODUCTION

Isogeometric analysis (IGA) is a method that integrates both design and analysis; engineers design models with the help of computer aided design (CAD) and the analysis of the design is done using Finite Element (FE). To capture complicated geometry accurately, generally NURBS basis functions are used along with the proper choice of control points. In this dissertation, IGA-Collocation method is presented to find numerical solution of partial differential equations containing singularities.

In Chapter 2, we review definitions and terminologies that are needed to understand this dissertation. Readers are suggested to read books such as Rogers [8], Piegl and Tiller [9] for more information. In section 2.2, three types of refinement methods are explained through examples. Section 2.3 gives the definition of Sobolev space and norm along with formula of norms which are used to do error analysis throughout this dissertation.

In Chapter 3, the basic IGA-Galerkin and IGA-Collocation approximation methods [25, 26] are presented and compared with an example. In section 3.2, several methods for construction of Partition of Unity (PU) functions are presented and used to enrich the region of singularity. Numerical results are shown in section 3.3. Also, the problem with oscillating singularity is tested in this section.

In Chapter 4, modification of basis functions are introduced so that $\mathcal{C}^0$-continuous functions can be made $\mathcal{C}^1$-continuous and then IGA-Collocation method can be used

to find the numerical solution of elliptic boundary value problems. In section 4.2, this method is extended to two dimensions. Section 4.3 presents a global basis numbering system which is used for assembling local stiffness matrices for two dimensional problems. In section 4.4, this method is tested for one as well as two dimensional problems.

In Chapter 5, the Schwarz alternating method in the framework of IGA-Collocation [27] is introduced. In section 5.1, the Schwarz alternating method is presented whereas in section 5.2, a parallel Schwarz method is presented. The results of numerical tests are shown in section 5.3.

In Chapter 6, an alternating method in the framework of IGA-Collocation is extended to two nonoverlapping subdomains. In section 6.1, the alternating method uses Dirichlet-Neumann boundary condition at the interface and in section 6.2 the method uses Neumann-Neumann boundary condition at the interface.

In Chapter 7, the Schwarz alternating iterative technique is explained for elasticity problems in the framework of IGA-Collocation. In section 7.1, a review of definitions and terminologies used in linear elasticity is explained. In section 7.2, the Schwarz alternating method is used to solve coupled elliptic equations using IGA-Collocation approach by splitting the problem into two overlapping subdomains. In section 7.3, this method is tested on non-singular as well as singular problems of elasticity.

Finally, concluding remarks and ongoing research are discussed in Chapter 8 of this dissertation.

CHAPTER 2: PRELIMINARIES

2.1 B-Splines and NURBS

This section provides definitions and terminologies that are needed to understand this dissertation. Readers are suggested to read books such as Rogers [8], Piegl and Tiller [9] for details.

2.1.1 B-Splines

A **knot vector** $U = \{u_1, u_2, ..., u_m\}$ is a non-decreasing sequence of real numbers in the parameter space $[0, 1]$, and the components u_i for $i = 1, 2, ..., m$ are called **knots**. An **open knot vector** of order $p + 1$ is a knot vector in which the first and the last knots are repeated $p + 1$ times. The interior knots can be repeated at most p times. For example,

$$\underbrace{u_1 = ... = u_{p+1}}_{p+1} < u_{p+2} \leq ... \leq u_{m-p-1} < \underbrace{u_{m-p} = ... = u_m}_{p+1}.$$

There are many ways to define B-spline basis functions. Here it is defined by the recurrence formula given by Cox-de Boor. The **B-spline basis functions** of order $k = p + 1$ corresponding to the knot vector U are piecewise polynomials of degree p, which are defined recursively in the following way

$$N_{i,1}(u) = \begin{cases} 1 & \text{if} \quad u_i \leq u < u_{i+1} \\ 0 & \text{otherwise} \end{cases} \tag{1}$$

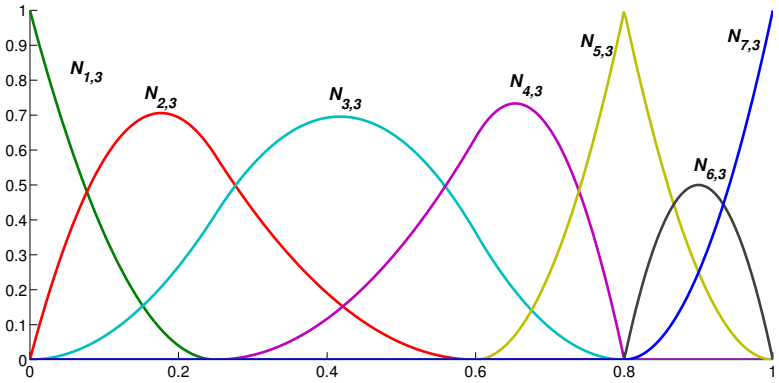

Figure 1: B-Spline functions $N_{i,3}(u), i = 1, 2, ..., 7$ of order $k = 3$ for knot vector $U = \{0, 0, 0, 0.25, 0.6, 0.8, 0.8, 1, 1, 1\}$

$$N_{i,t}(u) = \frac{u - u_i}{u_{i+t-1} - u_i} N_{i,t-1}(u) + \frac{u_{i+t} - u}{u_{i+t} - u_{i+1}} N_{i+1,t-1}(u) \tag{2}$$

where $1 \leq i \leq m - 1$ and $2 \leq t \leq k$. Fig. 1 shows B-spline basis functions corresponding to knot vector

$$U = \{0, 0, 0, 0.25, 0.6, 0.8, 0.8, 1, 1, 1\}.$$

B-Spline functions possess the following important properties:

1. $N_{i,k}(u)$ is non-negative for all i, k and u.

2. Each piecewise polynomial $N_{i,k}(u)$ has local support on $[u_i, u_{i+k})$.

3. On any span $[u_i, u_{i+1})$, at most $p + 1$ basis functions of degree p are non-zero.

   i.e. $N_{i-p,k}(u), N_{i-p+1,k}(u), N_{i-p+2,k}(u), ...,$ and $N_{i,k}(u)$.

4. The sum of all non-zero degree p basis functions on span $[u_i, u_{i+1})$ is 1.

5. B-Spline functions are linearly independent.

6. $N_{1,k}(0) = N_{m-1,k}(1) = 1$.

7. If the number of knots is m, then the number of B-spline basis functions of order k is $n = m - k$.

8. Basis function $N_{i,k}(u)$ is a composite curve of degree p polynomials with joining points at knots in $[u_i, u_{i+p+1})$.

9. The basis function $N_{i,k}(u)$ is $\mathcal{C}^{p-k}$-continuous at a knot of multiplicity k, .

A **B-spline curve** is defined as follows:

$$C(u) = \sum_{i=1}^{m-k} N_{i,k}(u) B_i, \tag{3}$$

where B_i are control points that make B-spline functions draw a desired curve. B-Spline curve and control points corresponding to open knot vector,

$$U = \{0, 0, 0, 0.25, 0.6, 0.8, 0.8, 1, 1, 1\}$$

are shown in Fig. 2. B-spline functions corresponding to the open knot vector of order $k = n + 1$:

$$U = \{\underbrace{0, 0, 0, ..., 0}_{n+1}, \underbrace{1, 1, 1, ..., 1}_{n+1}\}$$

are global polynomials, called Bézier polynomials. The B-spline curve obtained by Bézier polynomials is called the Bézier Curve. B-Spline curve possesses the following important properties:

1. A B-spline curve $C(u)$ is a union of curve segments where each component is a curve of degree p.

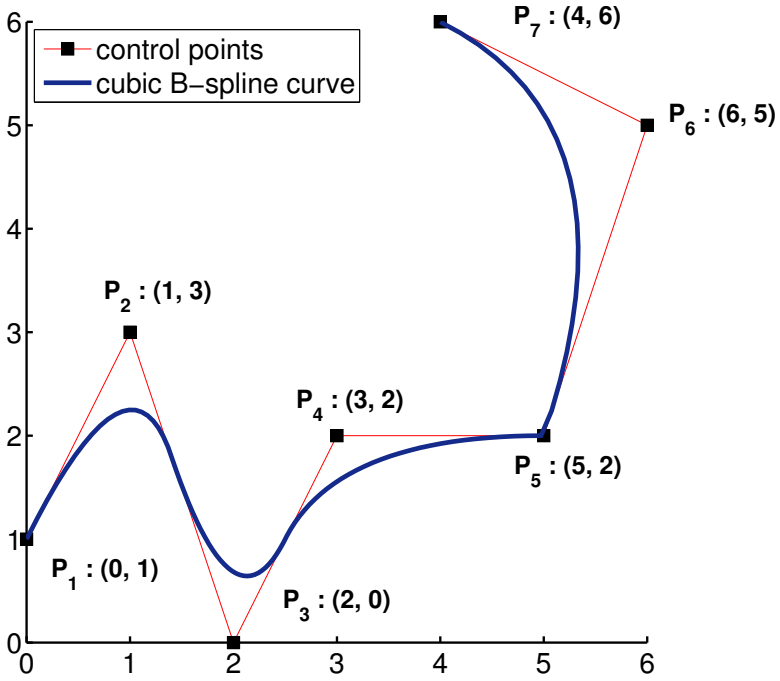

(a) B-Spline curve and control points

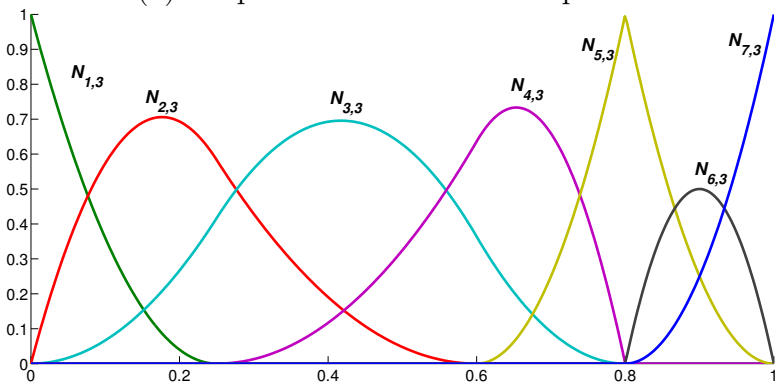

(b) B-Spline basis functions

Figure 2: (a) B-Spline curve and control points for open knot vector $U = \{0, 0, 0, 0.25, 0.6, 0.8, 0.8, 1, 1, 1\}$. (b) B-Spline basis functions corresponding to the B-Spline curve shown in (a)

2. A B-spline curve $C(u)$ satisfies the convex hull property, which means that the curve is contained in the convex hull of its control polyline. If u is in knot span $[u_i, u_{i+1})$, then $C(u)$ is in the convex hull of control points $B_{i-p}, B_{i-p+1}, ..., B_i$.

3. Changing the position of control point B_i only affects the curve $C(u)$ on interval $[u_i, u_{i+p+1})$.

4. A B-spline curve $C(u)$ is $\mathcal{C}^{p-k}$ continuous at a knot of multiplicity k.

5. If the curve is in a plane (or space), then no straight line (or plane) can intersect a B-spline curve more than it intersects the curve's control polyline. This property is called the *variation diminishing property* for B-spline curves.

6. B-spline curves also hold the *affine invariance property*, which means if an affine transformation is applied to a B-spline curve, then the result can be constructed from the affine images of its control points.

If there are knot vectors $U = \{u_1, u_2, u_3, ..., u_m\}$ and $V = \{v_1, v_2, v_3, ..., v_n\}$ in u and v-direction, respectively, then a **B-Spline surface** is defined by

$$S(u, v) = \sum_{i=1}^{m-k} \sum_{j=1}^{n-k'} N_{i,k}(u) M_{j,k'}(v) B_{i,j}, \tag{4}$$

where $N_{i,k}(u)$ and $M_{j,k'}(v)$ are B-Spline functions of degree p and degree q, respectively, and $B_{i,j}$ are control points that make a bidirectional control net as shown in Fig. 3.

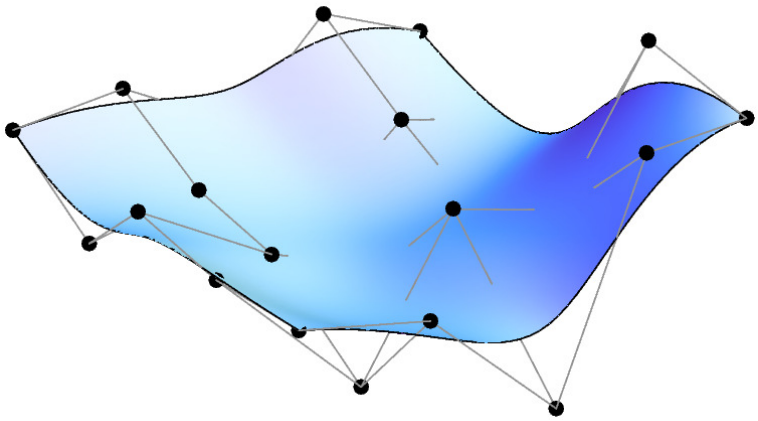

Figure 3: B-Spline surface and control net

2.1.2 NURBS

A **Non-Uniform Rational Basis Spline(NURBS)** function for the set of weights $\{w_i : i = 1, ..., m - k\}$ is defined by

$$R_{i,k}(u) = \frac{N_{i,k}(u)w_i}{W(u)}, \tag{5}$$

where

$$W(u) = \sum_{s=1}^{m-k} N_{s,k}(u)w_s > 0.$$

The NURBS basis functions are piecewise rational functions which possess the following properties:

1. $R_{i,k}(u)$ is non-negative for all i, k and u.

2. Each rational function $R_{i,k}(u)$ has local support on $[u_i, u_{i+k})$.

3. On any span $[u_i, u_{i+1})$, at most $p + 1$ basis functions of degree p are non-zero, if the weights are non-negative, i.e. $R_{i-p,k}(u), R_{i-p+1,k}(u), R_{i-p+2,k}(u), ...,$ and

$R_{i,k}(u)$.

4. The sum of all non-zero degree p basis functions on span $[u_i, u_{i+1})$ is 1.

5. NURBS basis functions are linearly independent.

6. If the number of knots is m, then the number of degree p basis functions is $n = m - k$.

7. NURBS basis function $R_{i,k}(u)$ is a composite curve of degree p rational functions with joining points at knots in $[u_i, u_{i+p+1})$.

8. At a knot of multiplicity k, basis function $R_{i,k}(u)$ is $\mathcal{C}^{p-k}$ continuous.

9. If $w_i = c$ for all i, where c is a non-zero constant, then $R_{i,k}(u) = N_{i,k}(u)$.

A **NURBS curve** for weights $w_i, i = 1, 2, ..., m - k$, and control points $B_i, i = 1, 2, ..., m - k$, is :

$$C(u) = \sum_{i=1}^{m-k} R_{i,k}(u) B_i, \tag{6}$$

as shown in Fig. 4.

NURBS curves possess the following important properties:

1. A NURBS curve $C(u)$ is a union of curve segments where each component is a rational curve of degree p.

2. A NURBS curve $C(u)$ satisfies the convex hull property.

3. Changing the position of control point B_i only affects the NURBS curve $C(u)$ on interval $[u_i, u_{i+p+1})$.

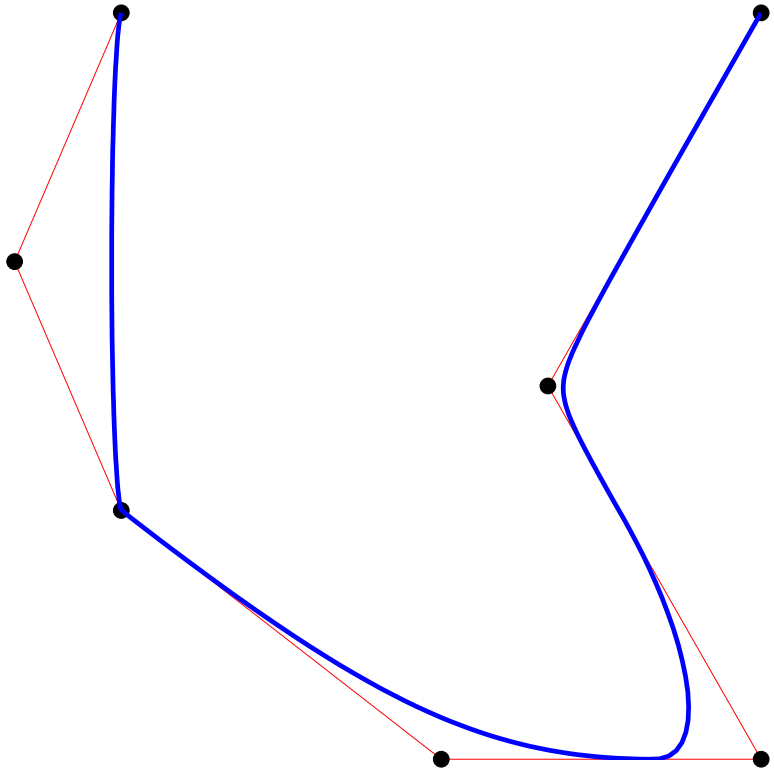

Figure 4: NURBS curve and control points

4. A NURBS curve $C(u)$ is C^{p-k} continuous at a knot of multiplicity k.

5. NURBS curves also hold the variation diminishing property.

6. NURBS curves do not hold the affine invariance property but they do hold the *projective invariance property*. If the projective transformation is applied to a NURBS curve, then the result can be constructed from the projective images of its control points.

If knot vectors $U = \{u_1, u_2, u_3, ..., u_m\}$ and $V = \{v_1, v_2, v_3, ..., v_n\}$ are in their respective u-direction and v-direction, then a **NURBS surface** corresponding to the control points $\{B_{i,j}\}$ and for the given set of weights $\{w_{i,j} : i = 1, ..., m - k, j =$

$1, ..., n - k'\}$ is defined by

$$S(u,v) = \sum_{i=1}^{m-k} \sum_{j=1}^{n-k'} \frac{N_{i,k}(u) M_{j,k'}(v) w_{i,j} B_{i,j}}{W(u,v)}, \tag{7}$$

where $N_{i,k}(u)$ and $M_{j,k'}(v)$ are NURBS basis functions of degree p and q, respectively.

2.2 Refinement

The B-spline basis can be enriched by three types of refinements: Knot insertion, degree elevation or degree and continuity elevation as shown in Figs. 5, 6, and 7, respectively. Knot insertion is equivalent to h-refinement in classical finite element method(FEM) and degree elevation is equivalent to p-refinement in classical FEM. Degree and continuity elevation does not exist in classical FEM.

2.2.1 Knot Insertion (h-refinement)

Knot insertion can be defined as, adding a new knot into the existing knot vector without changing the shape of the curve. This new knot may or may not be equal to an existing knot. If it is equal to an existing knot, then the multiplicity of that knot is increased by one.

In order to insert a new knot t into the knot vector $U = \{u_1, u_2, u_3, ..., u_m\}$ with m knots and n control points $\{P_1, P_2, ..., P_n\}$ without changing the shape of the B-spline curve $C(u)$, then the new knot vector will be given by $\overline{U} = \{\overline{u_1} = u_1, \overline{u_2} = u_2, ..., \overline{u_s} = t, ..., \overline{u_{m+1}} = u_m\}$. Suppose the new knot t lies in the knot span $[u_s, u_{s+1})$. The new control points Q_i will be given by

$$Q_i = (1 - a_i) P_{i-1} + a_i P_i, \tag{8}$$

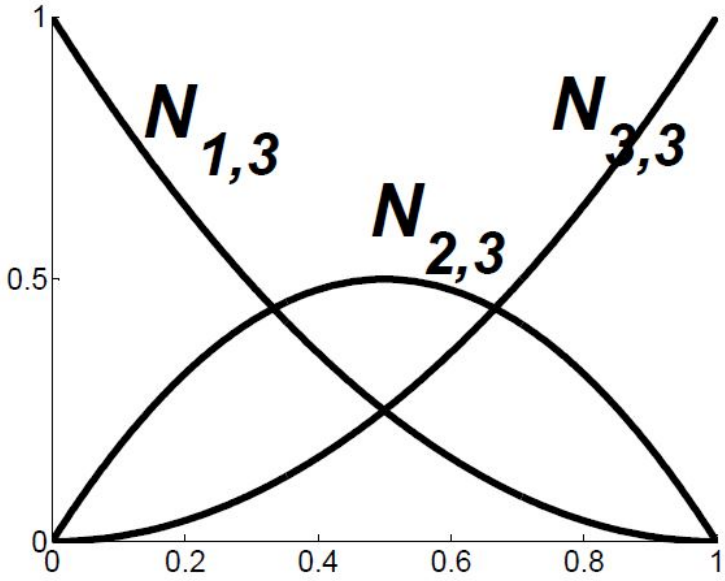

(a) Initial B-Spline function

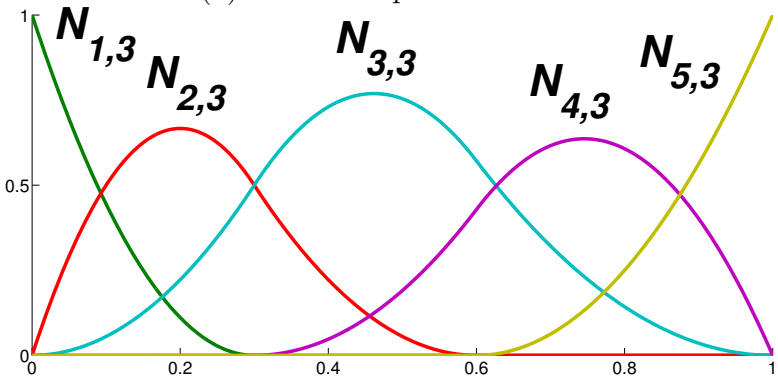

(b) B-Spline function after knot insertion

Figure 5: (a) Initial B-Spline basis function with knot vector $U = \{0, 0, 0, 1, 1, 1\}$. (b) B-Spline basis function after knot insertion with knot vector $U = \{0, 0, 0, \mathbf{0.3}, \mathbf{0.6}, 1, 1, 1\}$

where a_i can be calculated from

$$a_i = \begin{cases} 1 & \text{if} \quad i \leq s-p \\ \frac{t-u_i}{u_{i+p}-u_i} & \text{for} \quad s-p+1 \leq i \leq s \\ 0 & \text{if} \quad i \geq s+1. \end{cases} \tag{9}$$

2.2.2 Degree Elevation (p-refinement)

This refinement increases the degree of a curve without changing the shape of the curve. To keep the geometry and parametrization the same, the multiplicity of each knot is also increased by 1, if the degree is elevated by 1. This process preserves the discontinuities of various derivatives that are present in the original curve. Additionally, this method allows for a given surface to elevate in degrees in either the u-direction or the v- direction or both.

Assume a knot vector $\{u_1 = ... = u_{p+1} < u_{p+2} \leq ... \leq u_{m-p-1} < u_{m-p} = ... = u_m\}$ and n control points $\{P_1, P_2, ..., P_n\}$, in order to increase the degree of the curve by 1, without changing the shape of the B-spline curve $C(u)$, the new knot vector will be given by $\{u_1 = ... = u_{p+1} = u_{p+2} < u_{p+3} = u_{p+4} \leq ... \leq u_{2m-3p-4} = u_{2m-3p-3} < u_{2m-3p-2} = ... = u_{2m-2p-2}\}$ and the new control points Q_i will be given by

$$Q_i = \begin{cases} P_1 & \text{if} \quad i = 1 \\ \frac{(p+1-i)P_i+(i)P_{i-1}}{p+1} & \text{for} \quad 2 \leq i \leq p+1 \\ P_{p+1} & \text{if} \quad i = p+2. \end{cases} \tag{10}$$

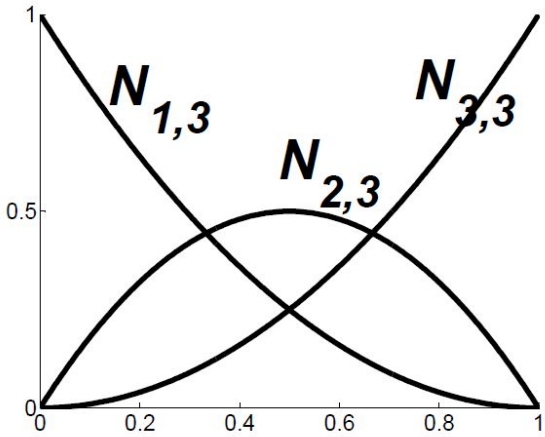

(a)Initial B-Spline function

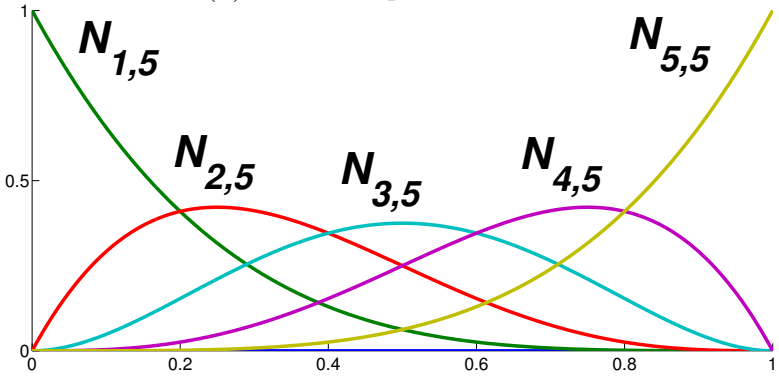

(b)B-Spline basis function after degree elevation

Figure 6: (a) Initial B-Spline function with knot vector $U = \{0, 0, 0, 1, 1, 1\}$. (b) B-Spline basis function after degree elevation with knot vector $U = \{0, 0, 0, 0, 0, 1, 1, 1, 1, 1\}$

2.2.3 k-refinement

This refinement comprises of both elevating the degree and inserting a new knot, without changing the shape of the curve. k-refinement has no equivalent refinement in finite element analysis (FEA). To do this refinement, the degree of the curve and the multiplicity of all intermediate knot values are increased so that the continuity of the curve does not change at these specific knots. Once prior is completed a new knot is inserted. These processes (Degree elevation and inserting knots) are not commutative and therefore the order in which these refinements are applied will change the final basis. Significant amounts of degrees of freedom can be saved by doing k-refinement.

Suppose the degree of initial knot vector $U = \{\underbrace{0,...,0}_{3}, 0.5, \underbrace{1,...,1}_{3}\}$ is to be increased from $p = 2$ to $p = 4$ and also a new knot $t = 0.6$ is to be inserted. If first degree elevation occurs, the knot vector becomes $U = \{\underbrace{0,...,0}_{5}, \underbrace{0.5,...,0.5}_{3}, \underbrace{1,...,1}_{5}\}$. Initially, the regularity of the curve at knot 0.5 was $\mathcal{C}^{2-1}$ which remains same $\mathcal{C}^{4-3}$ after degree elevation. Now inserting a new knot $t = 0.6$ gives knot vector $U = \{\underbrace{0,...,0}_{5}, \underbrace{0.5,...,0.5}_{3}, 0.6, \underbrace{1,...,1}_{5}\}$ which makes a total of 9 basis functions.

In case the order of degree elevation and knot insertion is reversed, then after the knot insertion of knot $t = 0.6$, the knot vector $U = \{\underbrace{0,...,0}_{3}, 0.5, \underbrace{1,...,1}_{3}\}$ changes to $U = \{\underbrace{0,...,0}_{3}, 0.5, 0.6, \underbrace{1,...,1}_{3}\}$ and after degree elevation from 2 to 4 it becomes $U = \{\underbrace{0,...,0}_{5}, \underbrace{0.5,...,0.5}_{3}, \underbrace{0.6,...,0.6}_{3}, \underbrace{1,...,1}_{5}\}$. This new knot vector gives a total of 11 basis functions whereas the previous k-refinement gave only 9 basis functions. New basis is completely different from the basis formed in the first case. Also, the first case will have less degrees of freedom than the second case.

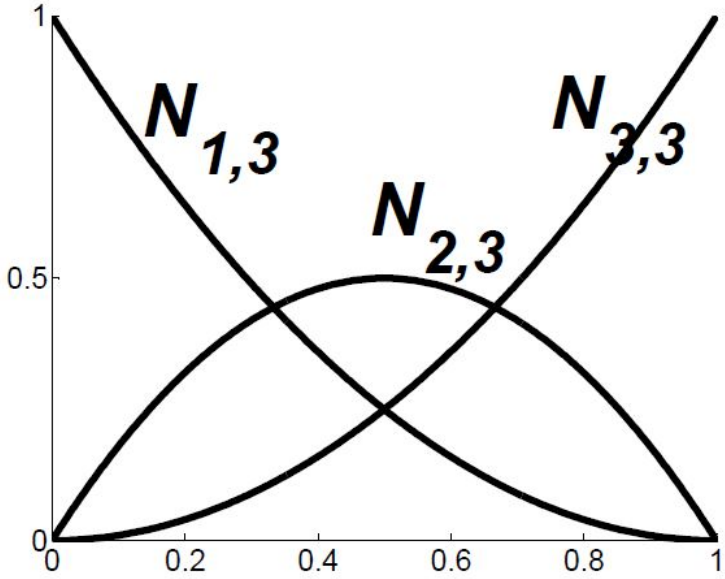

(a)Initial B-Spline function

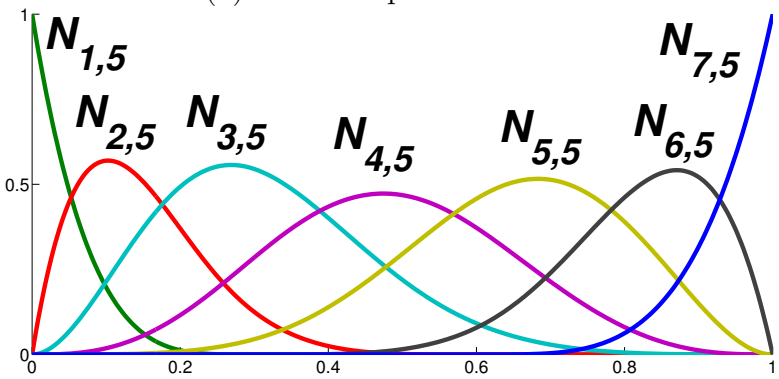

(b)B-Spline basis function after degree elevation

Figure 7: (a) Initial B-Spline function with knot vector $U = \{0, 0, 0, 1, 1, 1\}$. (b) B-Spline basis function after k-refinement with knot vector $U = \{0, 0, 0, 0, 0, 0.3, 0.6, 1, 1, 1, 1, 1\}$

2.3 Sobolev Space and Norm

In PDEs, solutions are calculated in Sobolev space. A **Sobolev space** is a vector space of functions equipped with a norm that is a combination of L^p-norms of the function itself and its derivatives up to a given order. The Sobolev space denoted by $W^{k,p}(\Omega)$, is the collection of u defined in Ω such that for every multi-index $\alpha = (\alpha_1, ..., \alpha_d)$ with $\mid \alpha \mid = \mid \alpha_1, ..., \alpha_d \mid \leq k$, the weak derivative $D^\alpha u$ exists and belongs to $L^p(\Omega)$. On $W^{k,p}(\Omega)$ we shall use the norm

$$\parallel u \parallel_{W^{k,p}(\Omega)} = \left(\sum_{|\alpha| \leq k} \int_\Omega |D^\alpha u|^p dx \right)^{\frac{1}{p}} \quad \text{if} \quad 1 \leq p < \infty. \tag{11}$$

For a real number $p \geq 1$, the p-norm or L^p-norm of $\mathbf{x}$ is defined by

$$\|\mathbf{x}\|_p = \left(|x_1|^p + |x_2|^p + \cdots + |x_n|^p\right)^{\frac{1}{p}}. \tag{12}$$

The L^∞-norm (or maximum norm) is the limit of the L^p-norms for $p \longrightarrow \infty$. This limit is equivalent to the following definition:

$$\|\mathbf{x}\|_\infty = \max\left\{|x_1|, |x_2|, \ldots, |x_n|\right\}. \tag{13}$$

The L^2-norm (or euclidean norm) is given by

$$\|\mathbf{x}\|_2 := \left(\sum_{i=1}^{n} |x_i|^2 \right)^{1/2}. \tag{14}$$

$H^{k,p}(\Omega)$ is defined by the completion of

$$\left\{ u \in \mathcal{C}^k(\Omega) | \parallel u \parallel_{W^{k,p}(\Omega)} < \infty \right\} \tag{15}$$

with respect to the norm $\|\cdot\|_p$, where $\mathcal{C}^k(\Omega)$ is consisting of all functions u which, together with all derivatives $D^\alpha(u)$ are continuous on Ω.

$$H^{k,p}(\Omega) \subset W^{k,p}(\Omega) \subset L^p(\Omega)$$

for all p. In particular, for $1 \leq p < \infty$, we have $H^{k,p}(\Omega) = W^{k,p}(\Omega)$.

In particular, when $p = 2$, we denote it as

$$W^{k,2}(\Omega) = W^k(\Omega) = H^k(\Omega).$$

$H_0^k(\Omega)$ is the closure of $C_0^\infty(\Omega)$ in the space $H^k(\Omega)$, where $C_0^\infty(\Omega)$ is the collection of infinitely differentiable functions with compact support in Ω.

2.3.1 Weak Solution in Sobolev Space

Let an integer $k \geq 0$, $\Omega \subset \mathcal{R}^d$ and $\alpha = (\alpha_1, ..., \alpha_d)$ for $u \in H^k(\Omega)$. The norm and the semi-norm, respectively, are defined by

$$\begin{aligned}
&\| u \|_{k,(\Omega)} = (\textstyle\sum_{|\alpha|\leq k} \int_\Omega |D^\alpha u|^2 dx)^{\frac{1}{2}}, \\
&\| u \|_{k,\infty,(\Omega)} = \max_{|\alpha|\leq k}\{\text{ess.sup} \mid D^\alpha u(x) \mid : x \in \Omega\}, \\
&| u |_{k,(\Omega)} = (\textstyle\sum_{|\alpha|=k} \int_\Omega |D^\alpha u|^2 dx)^{\frac{1}{2}}, \\
&| u |_{k,\infty,(\Omega)} = \max_{|\alpha|=k}\{\text{ess.sup} \mid D^\alpha u(x) \mid : x \in \Omega\}.
\end{aligned} \tag{16}$$

Given an elliptic boundary value problem on a domain Ω with Dirichlet boundary condition $g(x, y)$ along the boundary $\partial\Omega$, and let

$$\mathcal{W} = \{w \in H^1(\Omega) : w|_{\partial\Omega} = g\} \quad \text{and} \quad \mathcal{V} = \{w \in H^1(\Omega) : w|_{\partial\Omega} = 0\}. \tag{17}$$

The variational formulation of the Dirichlet boundary value problem can be written as follows: Find $u \in \mathcal{W}$ such that

$$\mathcal{B}(u, v) = \mathcal{L}(v), \quad \text{for all} \quad v \in \mathcal{V} \tag{18}$$

where $\mathcal{B}$ is a continuous bilinear form that is $\mathcal{V}$-elliptic [17] and $\mathcal{L}$ is a linear functional on $L_2(\Omega)$. The solution to (18) is called a **weak solution** which is equivalent to the strong (classical) solution that corresponds to an elliptic PDE whenever u is smooth enough. The energy norm of the trial function u is defined by

$$\|u\|_{eng} = \left[\frac{1}{2}\mathcal{B}(u, u)\right]^{\frac{1}{2}}. \tag{19}$$

Additionally, relative error in the energy norm(%) is calculated for some problems in this dissertation wherever IGA-Galerkin method is used to find numerical solution of the problem.

Since the NURBS basis functions do not satisfy the Kronecker delta property, therefore the non-homogeneous Dirichlet boundary condition is approximated by the least squares method as follows: $g^h \in \mathcal{W}^h$ such that

$$\int_{\partial\Omega} |g - g^h|^2 d\gamma = \text{minimum}. \tag{20}$$

Throughout this dissertation, the percentage relative error $\|\frac{u - u^h}{u}\|$ in the maximum norm(L^∞) as well as in the L^2 norm is defined by:

$$\|u - u^h\|_{\infty, rel(\%)} = \frac{\|u - u^h\|_\infty}{\|u\|_\infty} \times 100, \tag{21}$$

and

$$\|u - u^h\|_{L^2,rel(\%)} = \frac{\|u - u^h\|_{L^2}}{\|u\|_{L^2}} \times 100 \quad \text{respectively.} \tag{22}$$

CHAPTER 3: ENRICHED IGA-COLLOCATION

3.1 Isogeometric Analysis (IGA)

This chapter presents basic Galerkin and Collocation approximation methods in the framework of IGA for numerical solutions of PDEs. These methods are compared with the help of an example.

3.1.1 IGA-Galerkin Method

Consider the following two-dimensional model problem

$$\begin{cases} -\Delta u = f & \text{in} \quad \Omega, \\ u = 0 & \text{on} \quad \partial\Omega, \end{cases} \tag{23}$$

where $f \in L^2(\Omega)$. Domain Ω is a bounded connected open subset of $\mathcal{R}^2$ whose boundary $\partial\Omega$ is Lipschitz continuous.

Using Green's theorem we obtain the variational form of the model problem (23) as follows

$$\iint_\Omega (\nabla u)^T \nabla v d\Omega = \iint_\Omega f v d\Omega, \quad \text{for all} \quad v \in H_0^1(\Omega). \tag{24}$$

Suppose $\mathcal{V}_h$ is a finite dimensional subspace of $H_0^1(\Omega)$. Then the Galerkin approximation of (24) is to find $u_h \in \mathcal{V}_h$ such that

$$\iint_\Omega (\nabla u_h)^T \nabla v d\Omega = \iint_\Omega f v d\Omega, \quad \text{for all} \quad v \in \mathcal{V}_h. \tag{25}$$

Suppose the collection $\{\phi_1, \phi_2, ..., \phi_N\}$ is a basis for $\mathcal{V}_h$. Then for $u_h \in \mathcal{V}_h$ we have

$$u(x, y) \approx u_h(x, y) = \sum_{i=1}^{N} c_i \phi_i(x, y), \tag{26}$$

for some constants $\{c_1, c_2, ..., c_N\}$. Substituting (26) into (25) we have the following linear system for the unknown $\{c_1, c_2, ..., c_N\}$:

$$\sum_{j=1}^{N} c_j \iint_{\Omega} (\nabla \phi_i)^T \nabla \phi_j d\Omega = \iint_{\Omega} f \phi_i d\Omega, \quad \text{for} \quad i = 1, 2, ..., N. \tag{27}$$

Let,

$$\begin{cases} \iint_{\Omega} (\nabla \phi_i)^T \nabla \phi_j = a_{ij} \\ \iint_{\Omega} f \phi_i = b_i, \end{cases} \tag{28}$$

then the corresponding matrix equation for the unknown $\{c_1, c_2, ..., c_N\}$ is

$$\begin{pmatrix} a_{11} & a_{12} & \dots & a_{1N} \\ a_{21} & a_{22} & \dots & a_{2N} \\ \vdots & \vdots & \dots & \vdots \\ a_{N1} & a_{N2} & \dots & a_{NN} \end{pmatrix} \begin{pmatrix} c_1 \\ c_2 \\ \vdots \\ c_N \end{pmatrix} = \begin{pmatrix} b_1 \\ b_2 \\ \vdots \\ b_N \end{pmatrix}. \tag{29}$$

By solving (29) we obtain Galerkin approximate solution of (23) given by (26). When NURBS basis functions are used for Galerkin approximation, it is called *IGA-Galerkin method*.

3.1.2 IGA-Collocation Method

Suppose the right hand function $f(x, y)$ in (23) is continuous and $p_i = (x_i, y_i)$ is a point in $\Omega \subset \mathbf{R^2}$. For brevity, we write $x = (x, y), x_i = (x_i, y_i)$. If we use the Dirac δ

function $\delta(x - x_i)$ as a test function

$$\iint_{\Omega} (-\Delta u)\delta(x - x_i) = \iint_{\Omega} f\delta(x - x_i). \tag{30}$$

Then from the **shifting property** of the delta function we have,

$$(-\Delta u)(x_i) = f(x_i). \tag{31}$$

Suppose the basis functions $\{\phi_1, \phi_2, ..., \phi_N\}$ are $\mathcal{C}^1$-continuous, then by properly choosing N distinct points $\{p_1, p_2, ..., p_N\}$ in Ω, we obtain a system of linear equations:

$$-\Delta \left(\sum_{i=1}^{N} c_i \phi_i \right) (p_i) = f(p_i) \quad \text{for} \quad i = 1, 2, ..., N, \tag{32}$$

or,

$$-\sum_{i=1}^{N} c_i (\Delta \phi_i)(p_i) = f(p_i) \quad \text{for} \quad i = 1, 2, ..., N. \tag{33}$$

By solving the system in (33), one can determine the unknown coefficients $c_i, i = 1, 2, ..., N$. This method is called the **Collocation approximation method**.

The Collocation method using $\mathcal{C}^1$-continuous NURBS basis functions will be called **IGA-Collocation**. Even though the Collocation method has many advantages over the Galerkin method, the Collocation method has not been widely employed because of the complexity of constructions of $\mathcal{C}^1$-basis functions.

However, since highly smooth basis functions are used in IGA for numerical solutions of PDEs, the Collocation method starts to draw attention. The success of the Collocation method depends on not only constructing $\mathcal{C}^1$-continuous basis functions, but the proper choice of collocation points. Commonly used collocation points are

Greville abscissae of the knot vectors and *Gaussian quadrature* points.

Greville abscissae- The Greville abscissae $\bar{u}_i$ for the knot vector $U = \{u_1, u_2, u_3, ..., u_m\}$ can be found by the formula

$$\bar{u}_i = \frac{u_{i+1} + u_{i+2} + ... + u_{i+p}}{p}, 1 \leq i \leq m - k. \tag{34}$$

For example, the Greville abscissae of a knot vector $U = \{0, 0, 0, 0.5, 1, 1, 1\}$ are

$$\bar{u}_1 = 0, \quad \bar{u}_2 = \frac{1}{4}, \quad \bar{u}_3 = \frac{3}{4}, \quad \bar{u}_4 = 1.$$

Gaussian quadrature points: In numerical analysis, the quadrature rule is an approximation of the definite integral of a function, usually stated as a weighted sum of function values at specified points within the domain of integration. For the domain $[-1, 1]$ the rule is stated as

$$\int_{-1}^{1} f(x)dx \approx \sum_{i=1}^{n} w_i f(x_i) \tag{35}$$

where $w_i = \frac{2}{(1 - x_i)^2[P_n'(x_i)]^2}$, are the weights for Gauss-Legendre quadrature and x_i is the i-th root of Legendre polynomial $P_n(x)$, where by the Rodriquez formula, $P_n(x)$ is defined by

$$P_n(x) = \frac{1}{2^n n!} \frac{d^n}{dx^n}[(x^2 - 1)^n]. \tag{36}$$

These quadrature points are another choice for collocation points.

3.1.3 Comparison of IGA-Collocation with IGA-Galerkin Methods

In order to show the advantage of using IGA-Collocation over IGA-Galerkin, both methods are applied to the same elliptic boundary value problem with singularity of

type

$$r^{\lambda}\psi(\theta), \quad \text{where} \quad 0 < \lambda < 1, \text{and} \quad \psi \text{ is a smooth function.} \tag{37}$$

The problem discussed here has a singularity of type $r^{\frac{1}{2}}$ on a cracked circular domain of radius 1 and centered at origin.

$$\begin{cases} -\Delta u = f \quad \text{in} \quad \Omega = [(r,\theta) : r < 1, 0 < \theta < 2\pi] \\ u = 0 \quad \text{on} \quad \partial\Omega \end{cases} \tag{38}$$

with the exact solution given by:

$$u(r,\theta) = \sqrt{r}(1-r)\left[\sin\left(\frac{\theta}{2}\right) + \sin\left(\frac{3\theta}{2}\right)\right]. \tag{39}$$

Let F be a smooth mapping from the parameter space $\widehat{\Omega} = [0,1] \times [0,1]$ onto the physical space $\Omega = [(r,\theta) : r < 1, 0 < \theta < 2\pi]$ with crack along the positive x-axis, as shown in Fig. 8, is defined as follows:

$$F : \hat{\Omega} \to \Omega \quad \text{and} \quad F(u,v) = (x(u,v), y(u,v)),$$

where

$$F(u,v) = \begin{cases} x(u,v) = v^2 \cos(2\pi(1-u)) \\ y(u,v) = v^2 \sin(2\pi(1-u)). \end{cases} \tag{40}$$

This construction of mapping F generates singular functions. For IGA-Galerkin, the basis functions should be at least $\mathcal{C}^0$-continuous but for IGA-Collocation they have to be at least $\mathcal{C}^1$-continuous basis. Therefore we started with B-spline basis functions

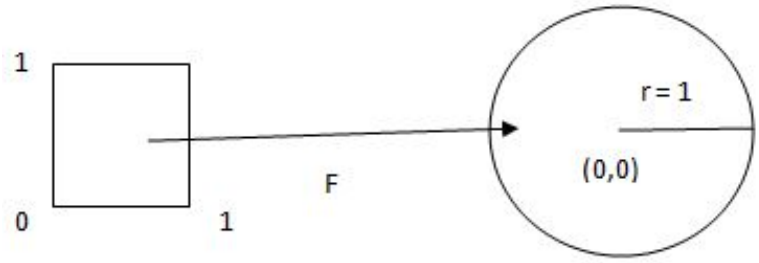

Figure 8: Mapping F maps $\widehat{\Omega} = [0,1] \times [0,1]$ onto physical space is $\Omega = [(r,\theta) : r < 1, 0 < \theta < 2\pi]$ with crack along the positive x-axis

corresponding to

$$\begin{aligned} U &= \{\underbrace{0,...,0}_{5}, \tfrac{1}{4}, \tfrac{1}{4}, \tfrac{1}{4}, \tfrac{1}{2}, \tfrac{1}{2}, \tfrac{1}{2}, \tfrac{3}{4}, \tfrac{3}{4}, \tfrac{3}{4}, \underbrace{1,...,1}_{5}\} \\ V &= \{\underbrace{0,...,0}_{4}, \underbrace{1,...,1}_{4}\} \end{aligned} \tag{41}$$

in u-direction and v-direction, respectively. To improve the isogeometric analysis of (38) in the angular direction we elevate the degree of B-spline functions with the fixed mesh size $h = \frac{1}{4}$ (the p-refinement). Relative errors in the maximum norm(%) for both IGA-Collocation and IGA-Galerkin are depicted in Table 1 and Fig. 9 whereas relative errors in the L^2-norm(%) for both methods are displayed in Table 2 and Fig. 10.

Table 3 and Fig. 11 show computation time for numerical solution of (38) obtained by IGA-Galerkin and IGA-Collocation methods. It is not difficult to see that as the degrees of freedom increases, the time taken by IGA-Collocation method increases linearly but for IGA-Galerkin method, the time increases almost exponentially. Therefore, when comparing IGA-Collocation with IGA-Galerkin with respect

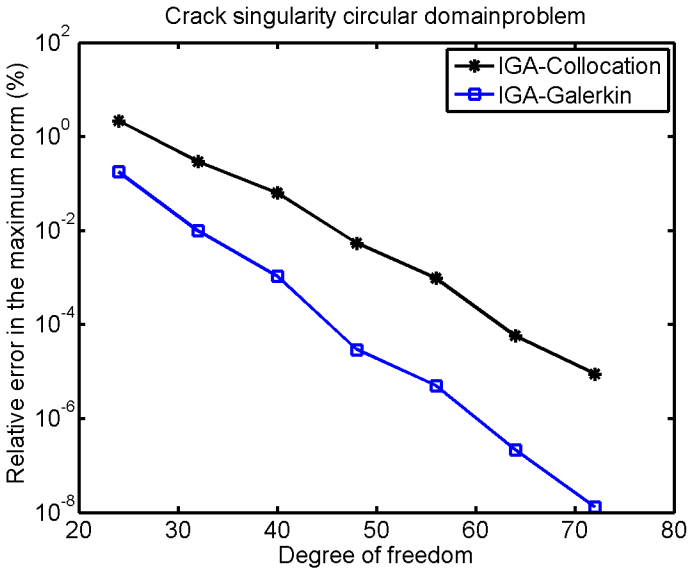

Figure 9: Comparison of relative errors in the max-norm(%) for numerical solutions obtained by IGA-Collocation and IGA-Galerkin methods for cracked singularity circular domain elliptic boundary value problem

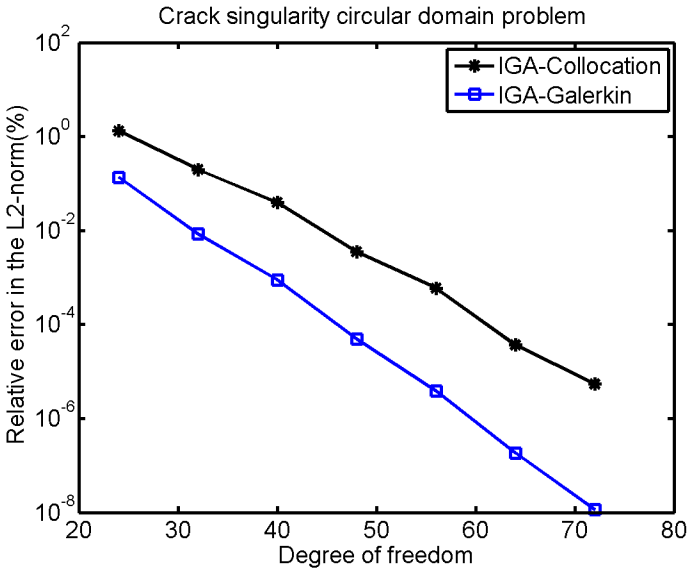

Figure 10: Comparison of relative errors in the L^2-norm(%) for numerical solutions obtained by IGA-Collocation and IGA-Galerkin methods for cracked singularity circular domain elliptic boundary value problem

Table 1: Comparison of relative errors in the max-norm(%) for numerical solutions obtained by IGA-Collocation and IGA-Galerkin methods for cracked singularity circular domain elliptic boundary value problem. Here (p_u, p_v) are degrees of B-spline functions

(p_u, p_v)	dof	IGA-Colloaction	IGA-Galerkin
$(4, 3)$	24	2.132E+00	1.756E-01
$(5, 3)$	32	2.916E-01	9.824E-03
$(6, 3)$	40	6.304E-02	1.062E-03
$(7, 3)$	48	5.360E-03	2.896E-05
$(8, 3)$	56	9.636E-04	4.976E-06
$(9, 3)$	64	5.731E-05	2.162E-07
$(10, 3)$	72	8.824E-06	1.319E-08

Table 2: Comparison of relative errors in the L^2-norm(%) for numerical solutions obtained by IGA-Collocation and IGA-Galerkin methods for cracked singularity circular domain elliptic boundary value problem. Here (p_u, p_v) are degrees of B-spline functions

(p_u, p_v)	dof	IGA-Colloaction	IGA-Galerkin
$(4, 3)$	24	1.314E+00	1.353E-01
$(5, 3)$	32	1.986E-01	8.378E-03
$(6, 3)$	40	3.939E-02	8.915E-04
$(7, 3)$	48	3.513E-03	4.922E-0-5
$(8, 3)$	56	5.945E-04	3.863E-06
$(9, 3)$	64	3.677E-05	1.849E-07
$(10, 3)$	72	5.403E-06	1.147E-08

to the cost of forming the stiffness matrix and the load vector, the cost of direct and iterative solvers, the degrees of freedom versus computing time, IGA-Collocation method has the potential to increase the computational efficiency of isogeometric analysis and to outperform IGA-Galerkin method, when a specified level of accuracy is to be achieved with minimum computational cost[23]. IGA-Collocation method provides huge time savings when considering large scale problems, even though the accuracy of the solution is two orders of magnitude less than IGA-Galerkin.

In problem (38), if instead of mapping F given by (40), another mapping G is used,

Table 3: Comparison of computation time (in seconds) for IGA-Galerkin and IGA-Collocation methods for the crack singularity problem

(p_u, p_v)	dof	IGA-Colloaction	IGA-Galerkin
$(4, 3)$	24	2.028	24.913
$(5, 3)$	32	3.042	49.561
$(6, 3)$	40	4.726	61.448
$(7, 3)$	48	7.456	142.833
$(8, 3)$	56	10.311	258.539
$(9, 3)$	64	12.947	335.385
$(10, 3)$	72	20.732	635.672

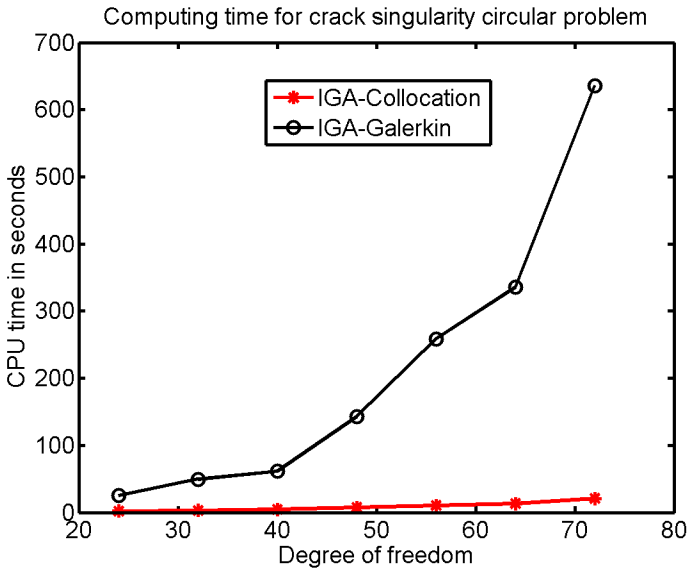

Figure 11: Comparison of computation time (in seconds) taken to obtain numerical solutions of problem (38) by IGA-Collocation and IGA-Galerkin methods

which is defined as follows:

$$G : \hat{\Omega} \to \Omega \quad \text{where} \quad G(u, v) = \begin{cases} x(u, v) = (v)\cos(2\pi(1-u)), \\ \\ y(u, v) = (v)\sin(2\pi(1-u)), \end{cases} \tag{42}$$

then this construction of mapping $G(u, v)$ will not generate singular functions. Problem (38) is solved with IGA-Collocation method in two different ways.

1. By using smooth mapping F which generates singular functions

1. By using mapping G which does not generate singular functions

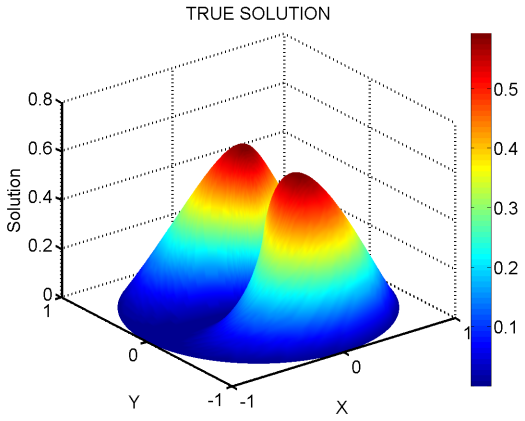

Figure 12: The true Solution given by (39)

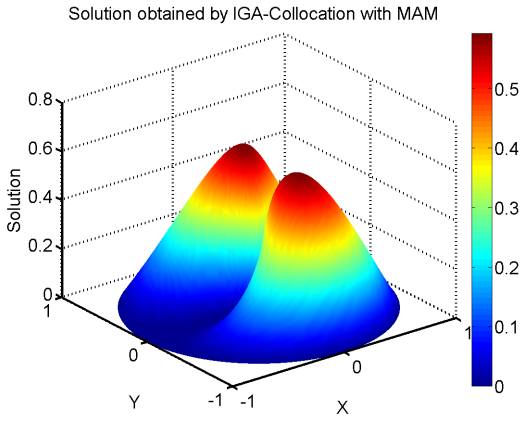

Figure 13: Numerical solutions obtained by IGA-Collocation with mapping technique

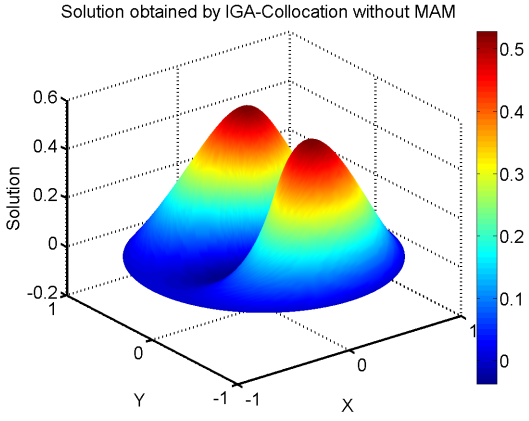

Figure 14: Numerical solutions obtained by IGA-Collocation without mapping technique

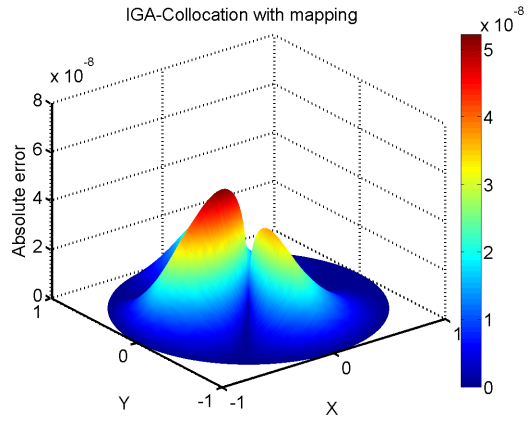

Figure 15: Absolute error obtained by IGA-Collocation with mapping technique

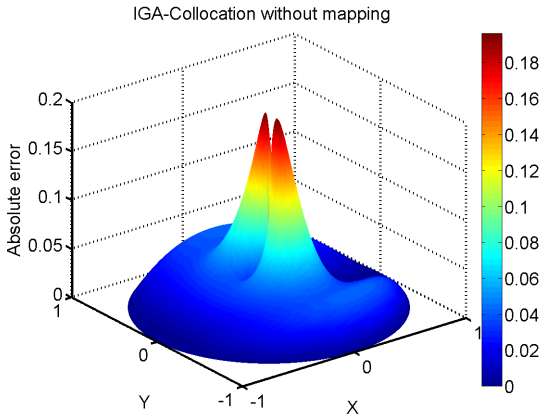

Figure 16: Absolute error obtained by IGA-Collocation without mapping technique

Absolute error(%) for both methods are shown in Figs. 15 and 16. IGA-Collocation with mapping techniques has absolute errors(%) upto 10^{-8} whereas without using mapping techniques absolute error(%) increases to 0.15. Figs. 12, 13 and 14 shows 3D-plots of true solution and solutions obtained by IGA-Collocation with mapping technique and IGA-Collocation without mapping technique.

3.2 Partition of Unity (PU) Functions

The following section will focus on Partition of Unity (PU) functions and their constructions. There are several ways to construct PU functions but only few which are applicable to implement in the framework of IGA-Collocation, are presented here. For this purpose, let us first introduce the notations and definitions.

Support: Let Ω denotes a bounded domain in $\mathbf{R^d}$. For $m \geq 0$, $C^m(\Omega)$ denotes the space of all functions ϕ with continuous derivatives upto order m. The support of ϕ is defined by

$$\text{supp } \phi = \overline{\{x \in \Omega : \phi(x) \neq 0\}}.$$

Partition of Unity: For Λ be a finite index set, a family $\{U_k : k \in \Lambda\}$ of open subsets of $\mathbf{R^d}$ is said to be a point finite open covering of $\Omega \subseteq \mathbf{R^d}$ if there is M such that any $x \in \Omega$ lies in at most M of the open sets U_k and $\Omega \subseteq \bigcup_k U_k$.

For a point finite open covering $\{U_k : k \in \Lambda\}$ of a domain Ω, suppose there is a family $\{\psi_k : k \in \Lambda\}$ of Lipschitz functions on Ω satisfying the following conditions:

1.For $k \in \Lambda, 0 \leq \psi_k(x) \leq 1, x \in \mathbf{R^d}$.

2. The supp$(\psi_k) \subseteq \overline{U_k}$, for each $k \in \Lambda$.

3. $\sum_{k \in \mathbf{D}} \psi_k(x) = 1$ for each $x \in \Omega$.

Then $\{\psi_k : k \in \Lambda\}$ is called a **partition of unity (PU)** subordinate to the covering $\{U_k : k \in \Lambda\}$. The covering sets U_k are called **patches**.

A **window (or weight) function** is a non-negative continuous function with compact support and is denoted by $\hat{w}(x)$. We consider the following conical window function in this dissertation: For $x \in \mathbf{R}$,

$$\hat{w}(x) = \begin{cases} (1-x^2)^l & \text{if} \quad \mid x \mid \leq 1, \\ 0 & \text{if} \quad \mid x \mid > 1 \end{cases} \tag{43}$$

where l is a positive integer. Then $\hat{w}(x)$ is a $\mathcal{C}^{l-1}$ function and it can be constructed from a one dimensional weight function as $w(x) = \prod_{i=1}^{d} \hat{w}(x_i)$, where $\mathbf{x} = (x_1, x_2, ..., x_d)$. **Normalized window functions** are defined by

$$\hat{w}_\delta^l(x) = A\hat{w}\left(\frac{x}{\delta}\right) \tag{44}$$

where $A = \dfrac{(2l+1)!}{2^{2l+1}(l!)^2\delta}$ is a constant that gives $\int_{\mathbf{R}} \hat{w}_\delta^l(x)dx = 1$.

1- **Shepard PU shape functions:**

Suppose window function is built at every particle x_i for each patch $w_i, i = 1, 2, ..., N$. Then the PU functions $\varphi_i(x)$ associated with particle $x_i, i = 1, 2, ..., N$ are defied by

$$\varphi_i(x) = \frac{w_i(x - x_i)}{\sum_k w_k(x - x_i)}, \quad \text{for all} \quad x \in \mathcal{R}. \tag{45}$$

2- **One-dimensional non-flat top PU functions[6]:**

This PU function is constructed by C^{n-1} piecewise polynomial $\varphi_n(x)$ for any

integer $n \geq 1$

$$\varphi_n(x) = \begin{cases} {\varphi^L}_n(x) := (1+x)^n g_n(x) & \text{if} \quad x \in [-1, 0] \\ {\varphi^R}_n(x) := (1-x)^n g_n(-x) & \text{if} \quad x \in [0, 1] \\ 0 & \text{otherwise} \end{cases} \tag{46}$$

where $g_n(x) = a_{0,n} + a_{1,n}(-x) + a_{2,n}(-x)^2 + ... + a_{n-1,n}(-x)^{n-1}$ is a polynomial of degree $n-1$. The coefficients $a_{k,n}$'s are defined by

$$a_{k,n}(x) = \begin{cases} 1 & \text{if} \quad k = 0 \\ \sum_{i=0}^{k} a_{i,n-1} & \text{if} \quad 0 < k \leq n-2 \\ 2a_{n-2,n} & \text{if} \quad k = n-1. \end{cases} \tag{47}$$

Using recurrence formula (46), $g_n(x)$ is computed as follows:

$$\begin{cases} g_1(x) = 1 \\ g_2(x) = 1 - 2x \\ g_3(x) = 1 - 3x + 6x^2 \\ g_4(x) = 1 - 4x + 10x^2 - x^3 \\ g_5(x) = 1 - 5x + 15x^2 - 35x^3 + 70x^4 \\ ..... \end{cases} \tag{48}$$

and so on. Since $\varphi_n(x)$ depends on both $(1+x)^n$ and $g_n(x)$ therefore $\varphi_n(x)$ is $\mathcal{C}^{n-1}$-continuous. Fig. 17 shows one-dimensional non flat top PU function.

3- **One-dimensional convolution flat-top PU functions[6]:**

Suppose domain $\Omega = [a, b]$ is partitioned uniformly (or non-uniformly) such that

$$x_1 = a - \delta < a < x_2 < ... < x_n < b < x_{n+1} = b + \delta. \tag{49}$$

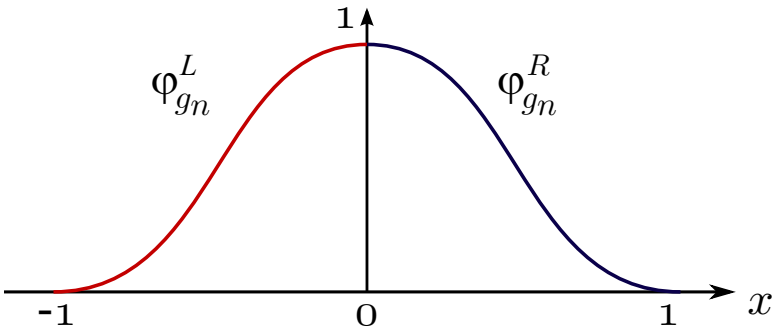

Figure 17: One-dimensional non-flat top PU function

Using non-flat PU functions we can construct PU functions with a flat top whose support is $[a-\delta, b+\delta]$ with $(a+\delta) < b-\delta$ in the following way:

$$\psi^{(\delta,n-1)}_{[a,b]}(x) = \begin{cases} \varphi^L_n\left(\frac{x-(a+\delta)}{2\delta}\right) & \text{if} \quad x \in [a-\delta, a+\delta] \\ 1 & \text{if} \quad x \in [a+\delta, b-\delta] \\ \varphi^R_n\left(\frac{x-(b-\delta)}{2\delta}\right) & \text{if} \quad x \in [b-\delta, b+\delta] \\ 0 & \text{if} \quad x \notin [a-\delta, b+\delta] \end{cases} \tag{50}$$

where φ^L_n and φ^R_n are defined by (46).

Here, in order to make a PU function to have a flat-top, we assume $\delta \leq \frac{(b-a)}{3}$. Actually, $\psi^{(\delta,n-1)}_{[a,b]}(x)$ is the convolution, $\chi_{Q_k}(x) * w^{n-1}_\delta$, of the characteristic function $\chi_{Q_k}(x)$ and the scaled window function w^{n-1}_δ, defined by (44). Let $Q_k = [x_k, x_{k+1}]$ be an interval with $\mid x_{k+1} - x_k \mid \geq 3\delta$ for $k = 1, 2, ..., n$. Then the characteristic function $\chi_{Q_k}(x)$ is defined by

$$\chi_{Q_k}(x) = \begin{cases} 1 \quad \text{if} \quad x \in [x_k, x_{k+1}], \\ 0 \quad \text{if} \quad x \notin [x_k, x_{k+1}]. \end{cases} \tag{51}$$

Since $\sum_{k=1}^n \chi_{Q_k}(x) = 1$, for all $x \in \Omega$ except for the nodal points, therefore $\sum_{k=1}^n \psi^{(\delta,n-1)}_k(x) = 1$ for all $x \in \Omega$. Fig. 18 shows one-dimensional convolution

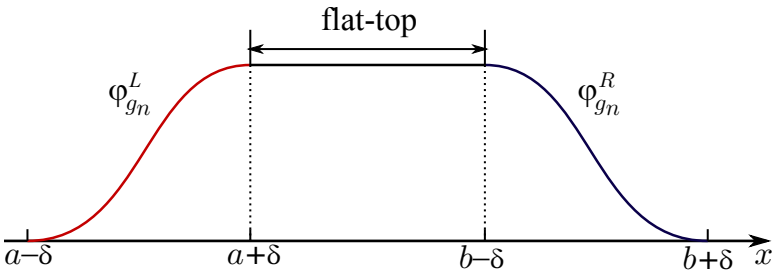

Figure 18: One-dimensional flat top PU function

flat-top PU function.

4- **Flat-top PU functions using B-Splines:**

To construct $\mathcal{C}^1$**-continuous PU functions with flat-top** using degree 3 B-spline functions $N_{i,4}(x), i = 1, \ldots, 12$ corresponding to knot vector

$$\Big\{\underbrace{0,..,0}_{4},\underbrace{a-\delta,a-\delta}_{2},\underbrace{a+\delta,a+\delta}_{2},\underbrace{b-\delta,b-\delta}_{2},\underbrace{b+\delta,b+\delta}_{2},\underbrace{1,..,1}_{4}\Big\}.$$

The non-flat top on the left side is constructed by,

$$\phi^L_{g_2}\left(\frac{x-(a+\delta)}{2\delta}\right) = N_{5,4}(x) + N_{6,4}(x) \quad \text{for} \quad x \in [a-\delta, a+\delta].$$

The non-flat top on the right side is constructed by,

$$\phi^R_{g_2}\left(\frac{x-(b-\delta)}{2\delta}\right) = N_{7,4}(x) + N_{8,4}(x) \quad \text{for} \quad x \in [b-\delta, b+\delta].$$

The flat portion of PU function is constructed by

$$N_{5,4}(x) + N_{6,4}(x) + N_{7,4}(x) + N_{8,4}(x) = 1 \quad \text{for} \quad x \in [a+\delta, b-\delta].$$

Similarly, to construct $\mathcal{C}^2$ **PU functions with flat-top** using degree 5 B-spline

functions $N_{i,6}(x), i = 1, \ldots, 18$, corresponding to knot vectors

$$\Big\{ \underbrace{0,..,0}_{6}, \underbrace{a-\delta,..,a-\delta}_{3}, \underbrace{a+\delta,..,a+\delta}_{3}, \underbrace{b-\delta,..,b-\delta}_{3}, \underbrace{b+\delta,..,b+\delta}_{3}, \underbrace{1,..,1}_{6} \Big\}$$

The non-flat top on the left side is constructed by,

$$\phi^L_{g3}\left(\frac{x-(a+\delta)}{2\delta}\right) = N_{7,6}(x) + N_{8,6}(x) + N_{9,6}(x) \quad \text{for} \quad x \in [a-\delta, a+\delta].$$

The non-flat top on the right side is constructed by,

$$\phi^R_{g3}\left(\frac{x-(b-\delta)}{2\delta}\right) = N_{10,6}(x) + N_{11,6}(x) + N_{12,6} \quad \text{for} \quad x \in [b-\delta, b+\delta].$$

The flat portion of PU function is constructed by

$$N_{7,6}(x)+N_{8,6}(x)+N_{9,6}(x)+N_{10,6}(x)+N_{11,6}(x)+N_{12,6}(x) = 1 \quad \text{for} \quad x \in [a+\delta, b-\delta].$$

Similarly, we construct general $\mathcal{C}^{n-1}$ **PU functions with flat-top** using degree 2n-1 B-spline functions $N_{i,2n}(x), i = 1, \ldots, 6n$, corresponding to knot vectors

$$\Big\{ \underbrace{0...0}_{2n}, \underbrace{a-\delta...a-\delta}_{n}, \underbrace{a+\delta...a+\delta}_{n}, \underbrace{b-\delta...b-\delta}_{n}, \underbrace{b+\delta...b+\delta}_{n}, \underbrace{1...1}_{2n} \Big\}$$

as follows:

$$\psi^{(\delta,n-1)}_{[a,b]}(x) = \begin{cases} \sum_{k=1}^{n} N_{2n+k,2n}(x) & \text{if} \quad x \in [a-\delta, a+\delta], \\ \sum_{k=1}^{2n} N_{2n+k,2n}(x) = 1 & \text{if} \quad x \in [a+\delta, b-\delta], \\ \sum_{k=1}^{n} N_{3n+k,2n}(x) & \text{if} \quad x \in [b-\delta, b+\delta], \\ 0 & \text{if} \quad x \notin [a-\delta, b+\delta]. \end{cases} \tag{52}$$

For example: To construct $\mathcal{C}^1$-continuous PU functions with flat-top using

degree 3 B-spline functions $N_{i,4}(x), i = 1, \ldots, 12$ corresponding to knot vector

$$U = \{\underbrace{0, ..., 0}_{4}, 0.35, 0.35, 0.4, 0.4, 0.6, 0.6, 0.65, 0.65, \underbrace{1, ..., 1}_{4}\}$$

This knot vector will have twelve cubic B-Spline functions in the $u-$direction with the following support:

$$\begin{aligned}
\text{Supp}(N_{1,4}(u)) = [0, 0.35], \quad \text{Supp}(N_{2,4}(u)) = [0, 0.35], \\
\text{Supp}(N_{3,4}(u)) = [0, 0.4], \quad \text{Supp}(N_{4,4}(u)) = [0, 0.4], \\
\text{Supp}(N_{5,4}(u)) = [0.35, 0.6], \quad \text{Supp}(N_{6,4}(u)) = [0.35, 0.6], \\
\text{Supp}(N_{7,4}(u)) = [0.4, 0.65], \quad \text{Supp}(N_{8,4}(u)) = [0.4, 0.65], \\
\text{Supp}(N_{9,4}(u)) = [0.6, 1], \quad \text{Supp}(N_{10,4}(u)) = [0.6, 1], \\
\text{Supp}(N_{11,4}(u)) = [0.65, 1], \quad \text{Supp}(N_{12,4}(u)) = [0.65, 1]
\end{aligned}$$

We will construct $\phi_i(u)$ function using the middle section of the B-Spline fucntions

$$\phi_i(u) = N_{5,4}(u) + N_{6,4}(u) + N_{7,4}(u) + N_{8,4}(u) = 1 \quad \text{if} \quad x \in [0.4, 0.6]. \quad (53)$$

Hence,

$$\phi_i(u) = \begin{cases} N_{5,4}(u) + N_{6,4}(u) & \text{if} \quad x \in [0.35, 0.4), \\ 1 & \text{if} \quad x \in [0.4, 0.6], \\ N_{7,4}(u) + N_{8,4}(u) & \text{if} \quad x \in (0.6, 0.65], \\ 0 & \text{otherwise.} \end{cases} \quad (54)$$

For two dimensional flat top PU function, let us consider knot vector $V =$

$\{\underbrace{0,...,0}_{4},0.2,0.2,0.3,0.3,\underbrace{1,...,1}_{4}\}$. There will be eight cubic B-Spline functions in the $v-$direction with the following support:

$$\begin{aligned}
&\text{Supp}(M_{1,4}(u)) = [0, 0.2], \quad \text{Supp}(M_{2,4}(u)) = [0, 0.2],\\
&\text{Supp}(M_{3,4}(u)) = [0, 0.3], \quad \text{Supp}(M_{4,4}(u)) = [0, 0.3],\\
&\text{Supp}(M_{5,4}(u)) = [0.2, 1], \quad \text{Supp}(M_{6,4}(u)) = [0.2, 1],\\
&\text{Supp}(M_{7,4}(u)) = [0.3, 1], \quad \text{Supp}(M_{8,4}(u)) = [0.3, 1].
\end{aligned}$$

We will construct $\phi_j(v)$ function using the first section of B-Spline functions as follows:

$$\phi_j(v) = M_{1,4}(v) + M_{2,4}(v) + M_{3,4}(v) + M_{4,4}(v) = 1 \quad \text{if} \quad x \in [0, 0.2]. \tag{55}$$

Hence,

$$\phi_j(v) = \begin{cases} 1 & \text{if} \quad x \in [0, 0.2], \\ M_{3,4}(v) + M_{4,4}(v) & \text{if} \quad x \in (0.2, 0.3), \\ 0 & \text{if} \quad x \in [0.3, 1]. \end{cases} \tag{56}$$

We can construct two-dimensional flat top PU function by taking tensor product of $\phi_i(u)$ and $\phi_j(v)$ functions as follows:

$$\psi_{i,j}(u, v) = \phi_i(u) \times \phi_j(v) = \sum_{i=5}^{8} \sum_{j=1}^{4} N_{i,4}(u) M_{j,4}(v). \tag{57}$$

It's not difficult to see that $\psi_{i,j}(u, v)$ is a unit function on the rectangle $[0.4, 0.6]\times$ $[0, 0.2]$.

3.3 Numerical Results

To show the effectiveness of the Partition of Unity IGA (PU-IGA) Collocation method it is tested to a second order boundary value problem (BVP) that has a singular solution.

3.3.1 Problem with Monotone Singularity of Type x^λ

Consider a model second order boundary value problem with singularity,

$$\begin{cases} -u''(x) = f & \text{for} \quad x \in (0,1) \\ u(0) = u(1) = 0 \end{cases} \tag{58}$$

with the exact solution:

$$u(x) = x^{1.7}(x-1). \tag{59}$$

Consider knot vector

$$U = \{0, 0, 0, 0.45, 0.5, 0.55, 1, 1, 1\}$$

for construction of $\mathcal{C}^1$-continuous PU functions with flat top. This knot vector will generate six quadratic B-Spline functions with the following supports:

$$\text{Supp}(N_{1,3}(u)) = [0, 0.45], \quad \text{Supp}(N_{2,3}(u)) = [0, 0.5],$$

$$\text{Supp}(N_{3,3}(u)) = [0, 0.55], \quad \text{Supp}(N_{4,3}(u)) = [0.45, 1],$$

$$\text{Supp}(N_{5,3}(u)) = [0.5, 1], \quad \text{Supp}(N_{6,3}(u)) = [0.55, 1].$$

Let $\phi_1(u)$ and $\phi_2(u)$ be $\mathcal{C}^2$-continuous PU functions constructed with the following B-spline functions:

$$\phi_1^L(u) = \begin{cases} 1 & \text{if} \quad x \in [0, 0.45), \\ N_{1,3}(u) + N_{2,3}(u) + N_{3,3}(u) & \text{if} \quad x \in [0.45, 0.55), \\ 0 & \quad x \in [0.55, 1], \end{cases} \tag{60}$$

and,

$$\phi_2^R(u) = \begin{cases} 0 & \text{if} \quad x \in [0, 0.45), \\ N_{4,3}(u) + N_{5,3}(u) + N_{6,3}(u) & \text{if} \quad x \in [0.45, 0.55), \\ 1 & \quad x \in [0.55, 1]. \end{cases} \tag{61}$$

These $\phi_1(u)$ and $\phi_2(u)$ are flat top PU-functions with non flat-tops on $[0.45, 0.55]$. Let

$$B_k(\xi) = \binom{n}{k}(1-\xi)^{n-k}\xi^k, k = 0, 1, 2, ...n$$

be Bernstein polynomials(Bézier functions) of degree n. Let $T_1 : [0, 1] \longrightarrow [0, 0.55]$ and $T_2 : [0, 1] \longrightarrow [0.45, 1]$ be bijective linear mappings. Construct $\mathcal{C}^2$-continuous basis functions on $[0, 0.55]$ and $[0.45, 1]$ as follows:

$$\mathcal{V}_1 = \{B_k(T_1^{-1}(x)) \times \phi_1(x) | k = 1, 2, ..., n_1\} \tag{62}$$

$$\mathcal{V}_2 = \{B_k(T_2^{-1}(x)) \times \phi_2(x) | k = 1, 2, ..., n_2\}. \tag{63}$$

Define an approximation space $\mathcal{V}$ on $[0, 1]$ by

$$\mathcal{V} = \text{span}(\mathcal{V}_1 \cup \mathcal{V}_2),$$

Table 4: The relative errors in the maximum norm in percentage for numerical solutions of one dimensional problem containing singularity obtained by enriched IGA-Collocation

Degree of 1st segment	Degree of 2nd segment	IGA-Collocation
$p = 6$	$p = 3$	5.10E-2
$p = 6$	$p = 6$	7.93E-3
$p = 10$	$p = 7$	1.46E-3

where $\mathcal{V}_1$ and $\mathcal{V}_2$ are approximation subspaces on $[0, 0.55]$ and $[0.45, 1]$, respectively. Divide domain $[0, 1]$ into two subdomains $[0, 0.55]$ and $[0.45, 1]$. Multiply each basis function in sudomain $[0, 0.55]$ by $\phi_1(u)$ and multiply each basis function in sudomain $[0.45, 1]$ by $\phi_2(u)$. Then the problem is solved using IGA-Collocation method for various combinations of degrees of basis functions in each subdomain. Relative errors in the maximum norm in percentage with respect to various combinations of p-degree in each segment are shown in Table 4.

3.3.2 An Elliptic Equation with Smooth Solution

Consider a second order boundary value problem containing no singularity.

$$\begin{cases} -u''(x) = f & \text{for} \quad x \in (0, 1) \\ u(0) = u(1) = 0 \end{cases} \tag{64}$$

with the exact solution:

$$u(x) = x^2(x - 1) \tag{65}$$

This elliptic boundary value problem containing a regular solution is solved in the same way the problem containing a weak singularity is solved. Relative errors in the maximum norm in percentage with respect to various combinations of p-degree are shown in Table 5.

Table 5: The relative errors in the maximum norm in percentage for numerical solutions of one dimensional non-singular problem obtained by enriched IGA-Collocation

Degree of 1st segment	Degree of 2nd segment	IGA-Collocation
$p = 6$	$p = 3$	2.01E-15
$p = 6$	$p = 6$	8.43E-16
$p = 10$	$p = 7$	1.59E-15

3.3.3 Problem with Oscillating Singularity

This test problem is on the domain [0,1]

$$\begin{cases} -u''(x) = f \qquad \text{for} \quad x \in (0,1) \\ u(0) = u(1) = 0 \end{cases} \tag{66}$$

with the exact solution:

$$u(x) = x^{0.65} \sin(0.1 \log x). \tag{67}$$

To solve this problem, domain [0,1] is divided into two overlapping subdomains [0, 0.55] and [0.45, 1]. An enrichment function $x^{0.65} \sin(0.1 \log x)$ is introduced in the singularity part to capture singularity. Define approximation space $\mathcal{V}$ in the following way:

$$\mathcal{V}_1^s = \{x^{0.65} \sin(0.1 \log x) \times \phi^L(x)\} \cup \mathcal{V}_1,$$

$$\mathcal{V} = \text{span}(\mathcal{V}_1^s \cup \mathcal{V}_2).$$

Relative errors in the maximum-norm(%) of the problem with oscillating singularity obtained by IGA-Collocation using enriched functions in $\mathcal{V}$ are displayed in Table 6 and Fig. 19.

Table 6: The relative errors in the maximum norm in percentage of numerical solutions of one dimensional second order equation with oscillating singularity obtained by IGA-Collocation

Degree of 1st segment	Degree of 2nd segment	DOF	IGA-Collocation
$p = 5$	$p = 6$	29	2.49E-07
$p = 5$	$p = 7$	30	9.63E-09
$p = 5$	$p = 8$	31	9.91E-10
$p = 5$	$p = 9$	32	1.91E-10
$p = 5$	$p = 10$	33	7.69E-12

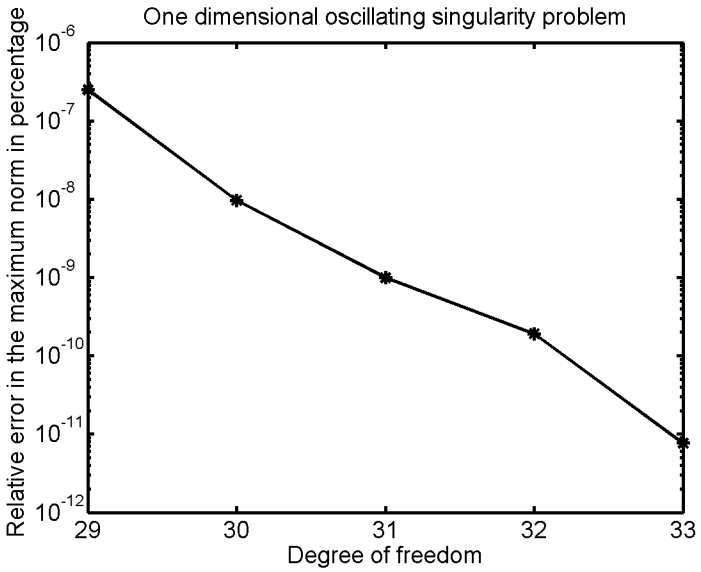

Figure 19: Relative errors in the max-norm(%) for oscillating singularity problem using IGA-Collocation method

CHAPTER 4: MODIFICATION OF BASIS FUNCTIONS

The basis functions used for the Collocation method should be $\mathcal{C}^1$-continuous, that means their derivatives should be continuous. If an elliptic boundary value problem is solved by the collocation method of an element-wise approach like in finite element method(FEM), then the basis functions must be modified at the patch to make them $\mathcal{C}^1$-continuous.

4.1 Modification of Bézier Polynomials in One-dimension

Suppose a physical domain is divided into several patches and assembles B-spline functions constructed on each patch in a patchwise manner. Then the derivatives of assembled B-spline functions could be discontinuous along the patch boundaries. To remove discontinuities of these derivatives of B-spline basis functions along these patch boundaries some modifications are necessary [18]. These modified B-spline functions are linearly independent and their first derivatives are zero at the first and the last knots, except for the second function and for the second last function.
By theorem 2.1 of [18], for $2 \leq k \leq n-1$ the first function $N_{1,n+1}(u)$ and the last function $N_{n+1,n+1}(u)$ can be altered as shown in Table 7 and these alterations are called **Nodal Alterations**. The alterations to the second function $N_{2,n+1}(u)$ and to the second last function $N_{n,n+1}(u)$ are called **Side Alterations**.

Applying this modifications to Bézier functions of degree 5 and taking $s = 2$, we

Table 7: Original and modified B-Spline basis functions

Index of B-spline function	Original function	Modified function
First function	$N_{1,k}(u)$	$N_{1,s}(u)(1+sx)$
Second function	$N_{2,k}(u)$	$-N_{2,k}(u)J(\phi)$
Preceding to last function	$N_{m-k-1,k}(u)$	$N_{m-k-1,k}(u)J(\phi)$
Last function	$N_{m-k,k}(u)$	$N_{m-k,s}(u)(1+s-sx)$

can get the following modified Bézier functions.

$$\begin{cases} N_{1,6}(u) = (1-u)^2(1+2u), \\ N_{2,6}(u) = -5u(1-u)^4 \left|J(\varphi_k(u))\right|, \\ N_{3,6}(u) = 10u^2(1-u)^3, \\ N_{4,6}(u) = 10u^3(1-u)^2, \\ N_{5,6}(u) = 5u^4(1-u) \left|J(\varphi_k(u))\right|, \\ N_{6,6}(u) = u^2(3-2u), \end{cases} \tag{68}$$

where $\varphi_k(u)$ is a linear patch mapping from the reference domain $\Omega = [0,1]$ to the physical subdomain $\Omega_k = [x_k, x_{k+1}]$ and $J(\varphi_k(u))$ is the Jacobian of $\varphi_k(u)$. The mapping $\varphi_k(u) : \Omega \to \Omega_k$ is defined by

$$\varphi_k(u) = (x_{k+1} - x_k)u + x_k. \tag{69}$$

4.2 Two-dimensional Extension of Modification

These modifications can be extended to two dimensional cases also. Consider mesh sizes $h_i = x_{i+1} - x_i$ and $k_j = y_{j+1} - y_j$ of $[a,b]$ and $[c,d]$, respectively. A two dimensional linear patch mapping $\varphi_{i,j}(u,v) : \Omega \to \Omega_{i,j}$ is defined by

$$\varphi_{i,j}(u,v) = \{h_i u + x_i, k_j v + y_j\} \tag{70}$$

Like the one dimensional case, we modify Bézier polynomials $N_{i,k}(u)$ and $M_{j,k'}(v)$ to get sets of modified Bézier basis functions in both u and v directions. Tensor product of these modified functions will give the reference shape functions for two dimensions. If we denote altered Bézier polynomials by $\tilde{N}_{i,k}(u)$ and $\tilde{M}_{j,k'}(v)$ and take degree 4 polynomials in both directions, then the tensor product will give us 25 reference shape functions.

$$\text{Nodal Alterations: } \begin{cases} \tilde{N}_{1,5}(u) \times \tilde{M}_{1,5}(v) & \tilde{N}_{1,5}(u) \times \tilde{M}_{5,5}(v), \\ \tilde{N}_{5,5}(u) \times \tilde{M}_{1,5}(v) & \tilde{N}_{5,5}(u) \times \tilde{M}_{5,5}(v). \end{cases} \tag{71}$$

$$\text{Side Alterations: } \begin{cases} \tilde{N}_{1,5}(u) \times \tilde{M}_{2,5}(v) & \tilde{N}_{1,5}(u) \times M_{3,5}(v) & \tilde{N}_{1,5}(u) \times M_{4,5}(v), \\ \tilde{N}_{2,5}(u) \times \tilde{M}_{1,5}(v) & N_{3,5}(u) \times \tilde{M}_{1,5}(v) & N_{4,5}(u) \times \tilde{M}_{1,5}(v), \\ \tilde{N}_{5,5}(u) \times \tilde{M}_{2,5}(v) & \tilde{N}_{5,5}(u) \times M_{3,5}(v) & \tilde{N}_{5,5}(u) \times M_{4,5}(v), \\ \tilde{N}_{2,5}(u) \times \tilde{M}_{5,5}(v) & N_{3,5}(u) \times \tilde{M}_{5,5}(v) & N_{4,5}(u) \times \tilde{M}_{5,5}(v). \end{cases} \tag{72}$$

$$\text{Internal Alterations: } \begin{cases} \tilde{N}_{2,5}(u) \times \tilde{M}_{2,5}(v) & \tilde{N}_{2,5}(u) \times M_{3,5}(v) & \tilde{N}_{2,5}(u) \times M_{4,5}(v), \\ N_{3,5}(u) \times \tilde{M}_{2,5}(v) & N_{3,5}(u) \times M_{3,5}(v) & N_{3,5}(u) \times M_{4,5}(v), \\ N_{4,5}(u) \times \tilde{M}_{2,5}(v) & N_{4,5}(u) \times M_{3,5}(v) & N_{4,5}(u) \times M_{4,5}(v). \end{cases} \tag{73}$$

4.3 Global Basis Numbering Used for Assembling Local Stiffness Matrices

When the modified Bézier polynomials of degree 4 are applied to an elliptic PDE on a rectangular domain consisting of nine rectangular patches, the numbering of global basis functions that are constructed by push-forwards of the 25 modified Bézier polynomials onto nine patches are as follows [18]:

$$
\begin{array}{cccccccccccc}
⑬ & 97 & 96 & 95 & ⑭ & 95 & 109 & 108 & ⑮ & 108 & 117 & 116 & ⑯ \\
98 & 103 & 104 & 105 & 94 & 105 & 112 & 113 & 107 & 113 & 120 & 121 & 115 \\
99 & 100 & 101 & 102 & 93 & 102 & 110 & 111 & 106 & 111 & 118 & 119 & 114 \\
69 & 74 & 75 & 76 & 65 & 76 & 83 & 84 & 78 & 84 & 91 & 92 & 86 \\
⑨ & 68 & 67 & 66 & ⑩ & 66 & 80 & 79 & ⑪ & 79 & 88 & 87 & ⑫ \\
69 & 74 & 75 & 76 & 65 & 76 & 83 & 84 & 78 & 84 & 91 & 92 & 86 \\
70 & 71 & 72 & 73 & 64 & 73 & 81 & 82 & 77 & 82 & 89 & 90 & 85 \\
26 & 35 & 36 & 37 & 22 & 37 & 49 & 50 & 42 & 50 & 62 & 63 & 55 \\
⑤ & 25 & 24 & 23 & ⑥ & 23 & 44 & 43 & ⑦ & 43 & 57 & 56 & ⑧ \\
26 & 35 & 36 & 37 & 22 & 37 & 49 & 50 & 42 & 50 & 62 & 63 & 55 \\
27 & 32 & 33 & 34 & 21 & 34 & 47 & 48 & 41 & 48 & 60 & 61 & 54 \\
28 & 29 & 30 & 31 & 20 & 31 & 45 & 46 & 40 & 46 & 58 & 59 & 53 \\
① & 17 & 18 & 19 & ② & 19 & 38 & 39 & ③ & 39 & 51 & 52 & ④
\end{array}
\tag{74}
$$

Here ⓚ represents the nodal basis function corresponding to the kth node.

Local numbering for the 25 shape functions listed in (71), (72), (73), is as follows:

$$
\begin{array}{ccccc}
④ & 13 & 12 & 11 & ③ \\
14 & 23 & 24 & 25 & 10 \\
15 & 20 & 21 & 22 & 9 \\
16 & 17 & 18 & 19 & 8 \\
① & 5 & 6 & 7 & ②
\end{array}
\tag{75}
$$

Here the shape functions listed in (71), (72), (73), respectively, are assigned the

following local numbers:

$$(Nodal)\begin{bmatrix} 4 & 3 \\ 1 & 2 \end{bmatrix}, \qquad (Side)\begin{bmatrix} 14 & 15 & 16 \\ 11 & 12 & 13 \\ 8 & 9 & 10 \\ 5 & 6 & 7 \end{bmatrix}, \qquad (Internal)\begin{bmatrix} 23 & 24 & 25 \\ 20 & 21 & 22 \\ 17 & 18 & 19 \end{bmatrix}.$$

4.4 Numerical Results

In this section, the numerical results of several one and two dimensional problems are presented, where the B-spline basis functions are modified to make them continuous at the patch boundaries.

4.4.1 One-dimensional Non-singular Problem

The first test problem is the Poisson equation on the domain [0,1]

$$\begin{cases} -u''(x) = f \qquad \text{for} \quad x \in (0,1), \\ u(0) = u(1) = 0, \end{cases} \tag{76}$$

with the exact solution:

$$u(x) = x^2(x-1). \tag{77}$$

This problem is numerically solved by using IGA-Collocation method. The basis functions corresponding to the following knot vector $U = \{\underbrace{0,...,0}_{7},\underbrace{1,...,1}_{7}\}$ are Bézier functions of degree 6. The physical domain [0,1] is first divided into 4 unequal size of mesh

$$[0,1] = \left[0,\frac{1}{8}\right] \cup \left[\frac{1}{8},\frac{1}{2}\right] \cup \left[\frac{1}{2},\frac{7}{8}\right] \cup \left[\frac{7}{8},1\right].$$

Table 8: Comparison of relative errors in the maximum norm in percentage for one dimensional problem (76) by using FEM-Galerkin and FEM-Collocation methods

Degree	FEM-Galerkin	FEM-Collocation
$p = 6$	9.36E-16	1.87E-15
$p = 7$	9.36E-16	5.24E-15
$p = 8$	1.49E-15	1.87E-15
$p = 9$	9.36E-16	4.21E-15
$p = 10$	1.12E-15	8.43E-16

Then the basis functions are modified at $\frac{1}{8}, \frac{1}{2}$ and $\frac{7}{8}$ to make them $\mathcal{C}^1$-continuous at these boundaries. Collocation points are chosen as Gauss quadrature points.

The relative errors in the max-norm(%) for the FEM-Collocation and the FEM-Galerkin methods for different degrees of basis functions are shown in Table 8. Both methods yield the solution of accuracy 10^{-15}, which is almost true solution. Note that increasing degree of Bézier polynomials will not make much difference so we can use less degrees of freedom(DOF) to get the same result.

4.4.2 One-dimensional Problem with Monotone Singularity of type x^λ

Consider the one-dimensional poisson equation,

$$\begin{cases} -u''(x) = f \qquad \text{for} \quad x \in (0,1) \\ u(0) = u(1) = 0 \end{cases} \tag{78}$$

that has the exact solution with weak singularity:

$$u(x) = x^{1.7}(x-1). \tag{79}$$

Like non singular problems, in this problem the physical domain [0,1] is also partitioned into four patches with unequal sizes and the basis functions are modified at these patch boundaries. The relative errors in the max-norm(%) for the FEM-

Table 9: Comparison of IGA-Galerkin and IGA-Collocation method for one dimensional singular problem

Degree	DOF	FEM-Galerkin	FEM-Collocation
$p = 6$	22	4.28E-05	3.32E-04
$p = 7$	26	2.49E-05	2.20E-04
$p = 8$	30	1.56E-05	1.24E-04
$p = 9$	34	1.05E-05	6.33E-05
$p = 10$	38	7.41E-06	4.21E-05

Collocation and the FEM-Galerkin methods for different degrees of basis functions are shown in Table 9. Both methods seem to have slow rate of convergence for the problem containing a weak singularity.

4.4.3 Two-dimensional Problem with No Singularity

Consider the two-dimensional Poisson equation on the domain $\Omega = \left[0, \frac{3}{2}\right] \times \left[0, \frac{3}{2}\right]$,

$$\begin{cases} -\Delta u = f & \text{in} \quad \Omega, \\ u = 0 & \text{on} \quad \partial\Omega, \end{cases} \tag{80}$$

with the exact solution:

$$u(x, y) = x^2 y^2 \left(x - \frac{3}{2}\right)\left(y - \frac{3}{2}\right). \tag{81}$$

To solve this 2-D problem, the physical domain $\left[0, \frac{3}{2}\right] \times \left[0, \frac{3}{2}\right]$ is partitioned into 3 equal sized patches in both directions resulting in a grid of 9 squares. The B-spline functions are modified in both u and v directions. We use $p = 4$ for numerical solutions of this problem. There are a total of 25 altered basis functions in each grid. The local stiffness matrix for each grid is created. Then the numbering technique mentioned in the previous section is followed to create the global stiffness matrix. In the FEM-Collocation method everything is calculated in the reference domain. Use

change of variables method to compute higher order derivatives in the following way: Consider a mapping $\Phi : \hat{\Omega} \to \Omega$ from the reference space to the physical space.

$$\hat{f} = f \circ \Phi, \quad \text{where } f(u, v) = (x, y).$$

By the chain rule,

$$\frac{\partial \hat{f}}{\partial u} = \frac{\partial f}{\partial x}\frac{\partial x}{\partial u} + \frac{\partial f}{\partial y}\frac{\partial y}{\partial u},$$
$$\frac{\partial \hat{f}}{\partial v} = \frac{\partial f}{\partial x}\frac{\partial x}{\partial v} + \frac{\partial f}{\partial y}\frac{\partial y}{\partial v}.$$

We have,

$$(\nabla_{xy} f) \circ \Phi = J(\Phi)^{-1} \nabla_{uv}(f \circ \Phi), \tag{82}$$

where $J_{11} = \dfrac{\partial x}{\partial u}; J_{12} = \dfrac{\partial y}{\partial u}; J_{21} = \dfrac{\partial x}{\partial v}; J_{22} = \dfrac{\partial y}{\partial v}$. For second derivative,

$$(\nabla_{xy} f_x) \circ \Phi = J(\Phi)^{-1} \nabla_{uv}(f_x \circ \Phi), (\nabla_{xy} f_y) \circ \Phi = J(\Phi)^{-1} \nabla_{uv}(f_y \circ \Phi). \tag{83}$$

Therefore,

$$f_{xx} \circ \Phi = J(\Phi)^{-1} \frac{\partial((J_{11})^{-1} \hat{f}_u + (J_{12})^{-1} \hat{f}_v)}{\partial u},$$
$$f_{xy} \circ \Phi = J(\Phi)^{-1} \frac{\partial((J_{11})^{-1} \hat{f}_u + (J_{12})^{-1} \hat{f}_v)}{\partial v},$$
$$f_{yx} \circ \Phi = J(\Phi)^{-1} \frac{\partial((J_{21})^{-1} \hat{f}_u + (J_{22})^{-1} \hat{f}_v)}{\partial u},$$
$$f_{yy} \circ \Phi = J(\Phi)^{-1} \frac{\partial((J_{21})^{-1} \hat{f}_u + (J_{22})^{-1} \hat{f}_v)}{\partial v}.$$

Since the inverse mapping $\Phi^{-1} : \Omega \to \hat{\Omega}$

$$f = \hat{f} \circ \Phi^{-1},$$

Table 10: Comparison of FEM-Galerkin and FEM-Collocation for a two dimensional problem with no singularity

Method	degree	$\|u-u^h\|_{\infty,rel(\%)}$	$\|u-u^h\|_{L^2,rel(\%)}$	$\|u-u^h\|_{eng,rel(\%)}$
IGA-Galerkin	$p=4$	1.44E-15	6.06E-14	1.74E-06
IGA-Collocation	$p=4$	5.76E-13	1.21E-12	N/A

$$
\begin{aligned}
(\partial_{xx} f)\circ\Phi &= (J_{11})^{-1}\frac{\partial}{\partial u}\left\{(J_{11})^{-1}\frac{\partial}{\partial u}\hat{f}+(J_{12})^{-1}\frac{\partial}{\partial v}\hat{f}\right\}\\
&+ (J_{12})^{-1}\frac{\partial}{\partial v}\left\{(J_{11})^{-1}\frac{\partial}{\partial u}\hat{f}+(J_{12})^{-1}\frac{\partial}{\partial v}\hat{f}\right\},
\end{aligned}
$$

$$
\begin{aligned}
(\partial_{yy} f)\circ\Phi &= (J_{21})^{-1}\frac{\partial}{\partial u}\left\{(J_{21})^{-1}\frac{\partial}{\partial u}\hat{f}+(J_{22})^{-1}\frac{\partial}{\partial v}\hat{f}\right\}\\
&+ (J_{22})^{-1}\frac{\partial}{\partial v}\left\{(J_{21})^{-1}\frac{\partial}{\partial u}\hat{f}+(J_{22})^{-1}\frac{\partial}{\partial v}\hat{f}\right\},
\end{aligned}
$$

$$
\begin{aligned}
(\partial_{xy} f)\circ\Phi &= (J_{21})^{-1}\frac{\partial}{\partial u}\left\{(J_{11})^{-1}\frac{\partial}{\partial u}\hat{f}+(J_{12})^{-1}\frac{\partial}{\partial v}\hat{f}\right\}\\
&+ (J_{22})^{-1}\frac{\partial}{\partial v}\left\{(J_{11})^{-1}\frac{\partial}{\partial u}\hat{f}+(J_{12})^{-1}\frac{\partial}{\partial v}\hat{f}\right\},
\end{aligned}
$$

$$
\begin{aligned}
(\partial_{yx} f)\circ\Phi &= (J_{11})^{-1}\frac{\partial}{\partial u}\left\{(J_{21})^{-1}\frac{\partial}{\partial u}\hat{f}+(J_{22})^{-1}\frac{\partial}{\partial v}\hat{f}\right\}\\
&+ (J_{12})^{-1}\frac{\partial}{\partial v}\left\{(J_{21})^{-1}\frac{\partial}{\partial u}\hat{f}+(J_{22})^{-1}\frac{\partial}{\partial v}\hat{f}\right\},
\end{aligned}
$$

$$\Delta_{xy} f\circ\Phi = \Delta_{xy}(\hat{f}\circ\Phi^{-1})\circ\Phi = (\partial_{xx} f)\circ\Phi + (\partial_{yy} f)\circ\Phi.$$

The model two-dimensional problem is solved by both the FEM-Galerkin and the FEM-Collocation methods. The relative errors in the maximum norm(%) and L^2-norm(%) for both methods are displayed in Table 10.

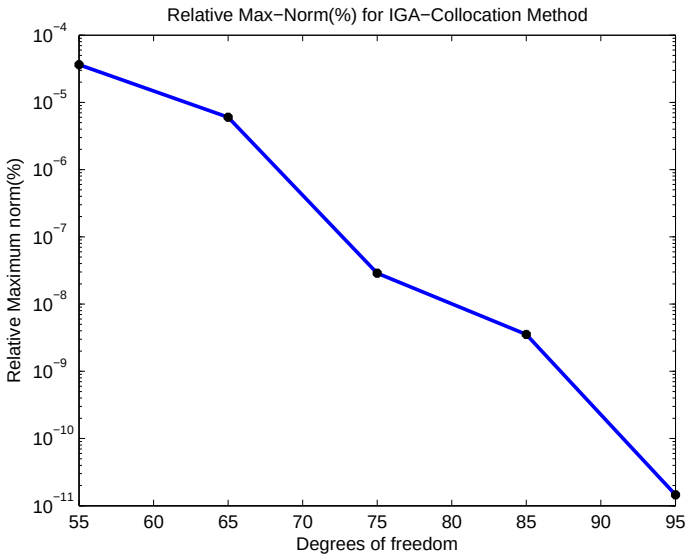

Figure 20: Relative errors in the max-norm(%) of numerical solutions obtained by IGA-Collocation for Problem (84)

4.4.4 Two-dimensional Problem with Singularity

Consider the Poisson equation on the semi-circular domain of radius 1/2 and centered at origin.

$$\begin{cases} -\Delta u = f \quad \text{in} \quad \Omega \\ u = 0 \quad \text{on} \quad \partial\Omega \end{cases} \tag{84}$$

that has the exact solution:

$$u(r,\theta) = \sqrt{r}\left(\frac{1}{2} - r\right)\sin\theta. \tag{85}$$

To map the reference domain onto the physical domain, smooth non-NURBS mapping $F : \hat{\Omega} \to \Omega$ is used where

$$F(u,v) = \begin{cases} x(u,v) = \frac{(v^2)}{2}\cos(\pi(1-u)) \\ y(u,v) = \frac{(v^2)}{2}\sin(\pi(1-u)). \end{cases} \tag{86}$$

Table 11: Relative errors(%) of numerical solutions obtained by applying IGA-Collocation method to two-dimensional Poisson equation on a semicircular domain with singularity

(p_u, p_v)	$\|u - u^h\|_{\infty,rel(\%)}$	$\|u - u^h\|_{L^2,rel(\%)}$
(6,3)	3.63E-05	3.08E-05
(7,3)	6.02E-06	4.26E-06
(8,3)	2.88E-08	1.75E-08
(9,3)	3.54E-09	2.45E-09
(10,3)	1.45E-11	8.64E-12

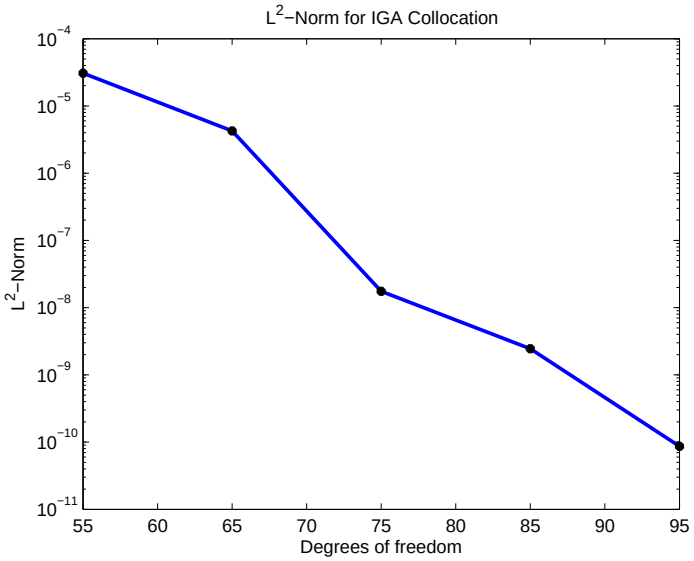

Figure 21: Relative errors in the L^2-norm(%) of numerical solutions obtained by the IGA-Collocation for Problem (84)

The degree of the Bézier functions in v direction is fixed to 3 whereas the degree in u direction is elevated. Modified Bézier polynomials are used as basis functions. The relative errors in the max-norm(%) and in the L^2-norm(%) are depicted in Table 11. Figs. 20 and 21 graph the columns of Table 11.

CHAPTER 5: SCHWARZ ALTERNATING METHOD IN THE FRAMEWORK OF IGA-COLLOCATION

The Schwarz alternating method was introduced by H. A. Schwarz[19] in 1870. A modification of this method is known as the parallel Schwarz method. In the Schwarz alternating method, the domain is divided into two overlapping subdomains and the iterative procedure starts by taking one initial guess for the boundary of first subproblem. This method involves solving the boundary value problem on each of the two subdomains in turn, taking always the last values of the approximated solution as the next boundary condition for artificial boundaries crested by this subdivision. It is important to note that in the Schwarz alternating method, the solution of the first problem is required before the second problem can be solved. In the parallel Schwarz method, the domain is divided into two overlapping subdomains and the iterative procedure starts by taking initial guesses on each subdomain. In this case the subproblem can be solved independently in each subdomain.

5.1 Schwarz Alternating Method

The classical Schwarz alternating method in the framework of IGA-Collocation is explained in this section. Consider the Poisson problem

$$\begin{cases} -\Delta u = f \quad \text{in} \quad \Omega, \\ u = 0 \quad \text{on} \quad \partial\Omega, \end{cases} \tag{87}$$

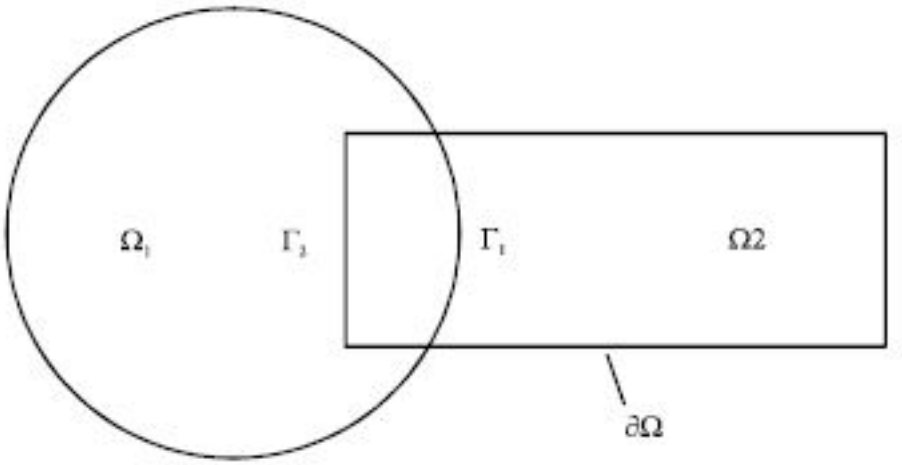

Figure 22: Overlapping subdomains with artificial boundaries

on a bounded Lipschitz region Ω with homogeneous boundary condition on boundary $\partial\Omega$. The physical domain Ω is divided into two subdomains Ω_1 and Ω_2 with artificial boundaries Γ_1 and Γ_2, respectively, as shown in Fig. 22. Define $\phi_i(x, y)$ and $\phi_j(x, y)$ basis functions for subdomains Ω_1 and Ω_2, respectively. Assume,

$$u_1(x, y) \approx u_h(x, y) = \sum_{i=1}^{N} c_i \phi_i(x, y), \tag{88}$$

$$u_2(x, y) \approx v_h(x, y) = \sum_{j=1}^{M} c_j \phi_j(x, y). \tag{89}$$

In IGA-Collocation method, $\phi_i(x, y)$ and $\phi_j(x, y)$ are NURBS basis functions.

This subdivision provides two subproblems to solve using IGA-Collocation method[22].

$$\begin{cases} -\Delta u_1^{n+1} = f \quad \text{for} \quad \Omega_1 \\ u_1^{n+1} = 0 \quad \text{on} \quad \partial\Omega_1 \setminus \Gamma_1 \\ u_1^{n+1} = u_2^n \quad \text{on} \quad \Gamma_1 \end{cases} \tag{90}$$

$$\begin{cases} -\Delta u_2^{n+1} = f \quad \text{for} \quad \Omega_2 \\ u_2^{n+1} = 0 \quad \text{on} \quad \partial\Omega_2 \setminus \Gamma_2 \\ u_2^{n+1} = u_1^{n+1} \quad \text{on} \quad \Gamma_2 \end{cases} \tag{91}$$

where n denotes the number of iterations. To start the iterative process, subproblem(90) is first solved for $n = 0$ with some initial guess $u_2^0 = g(x, y)$ on the artificial boundary Γ_1. Then the subproblem (91) is solved by using the solution obtained in subproblem (90) for the artificial boundary Γ_2.

Problem(87) is solved by iterating steps (90) and (91) while updating $u_1^{n+1}(x, y)$ and $u_2^{n+1}(x, y)$ with the most updated values of $u_2(x, y)$ and $u_1(x, y)$, respectively, at the artificial boundaries Γ_1 and Γ_2. The iterations are performed until certain convergence conditions are met. The least squares method is used to determine unknowns c_i's and c_j's along the artificial boundaries Γ_1 and Γ_2.

5.2 The Parallel Schwarz Method

Pierre-Louis Lions [20] proposed the parallel Schwarz method by doing small but essential modification in the Schwarz alternating method which made the problem perfect for parallel computing. Lions modified subproblems (90)-(91) in the following way:

$$\begin{cases} -\Delta u_1^{n+1} = f \quad \text{for} \quad \Omega_1 \\ u_1^{n+1} = 0 \quad \text{on} \quad \partial\Omega_1 \setminus \Gamma_1 \\ u_1^{n+1} = u_2^{n} \quad \text{on} \quad \Gamma_1 \end{cases} \tag{92}$$

$$\begin{cases} -\Delta u_2^{n+1} = f \quad \text{for} \quad \Omega_2 \\ u_2^{n+1} = 0 \quad \text{on} \quad \partial\Omega_2 \setminus \Gamma_2 \\ u_2^{n+1} = u_1^n \quad \text{on} \quad \Gamma_2 \end{cases} \tag{93}$$

To start this parallel process, subproblems (92)-(93) are solved together for $n = 0$ step with two initial guesses $u_2^0 = g(x, y)$ and $u_1^0 = h(x, y)$ on the artificial boundaries Γ_1 and Γ_2, respectively. In this method, both subproblems are solved simultaneously at each step. To get solution at $(n + 1)$th step solutions of both subproblems are required at n-th step.

5.3 One-dimensional Problems

Several problems are tested in one-dimensional cases, to see the efficiency of the iterative method using IGA-Collocation. Performance tests are conducted using the Schwarz alternating method with respect to the following three combinations:

[I] IGA-Galerkin on Ω_1 and IGA-Galerkin on Ω_2

[II] IGA-Galerkin on Ω_1 and IGA-Collocation on Ω_2

[III] IGA-Collocation on Ω_1 and IGA-Collocation on Ω_2

5.3.1 One-dimensional Problems Whose Solutions are Smooth

Consider the one dimensional Poisson equation

$$\begin{cases} -u''(x) = f \quad \text{in} \quad \Omega \\ u(x) = 0 \quad \text{on} \quad \partial\Omega \end{cases} \tag{94}$$

Table 12: Various overlapping sizes, number of iterations, ratio of relative errors and slope of line of convergence for problem(94)

Overlapping Size	0.1	0.2	0.3	0.4	0.5	0.6	0.7	0.8	0.9
Iterations	51	26	17	13	10	8	6	5	3
$(err2/err1)$	0.66	0.44	0.29	0.17	0.11	0.05	0.03	0.01	0.002
$\lambda \approx \frac{\log(err2/err1)}{N_2 - N_1}$	-0.42	-0.82	-1.24	-1.77	-2.21	-2.99	-3.51	-4.61	-6.21

with a smooth solution:

$$u(x) = x^2 - x^3 \tag{95}$$

Problem (94) is solved with respect to various sizes of the overlapping subdomains with an initial guess 0 on the artificial boundary Γ_1. Relative errors in the maximum norm(%) versus the sizes of overlapping subdomains are depicted in Fig. 23. Table 12 shows that the larger the overlapping subdomains are, the less the number of iterations are.

The location of artificial boundaries does not matter for the rate of convergence when the solution is smooth. If the size of the overlapping region is increased, then the solution acquired in the first step is very close to the true solution, which requires fewer iterations, and thus resulting in a smaller convergence rate as shown in Table 12. Since relative errors versus the number of iterations on a semi-log scale are straight lines for various sizes of overlapping subdomains, we expect the following lemma:

Theorem- *Let N be the number of iterations in the alternating method and $\|err\|_\infty$ be the relative errors in the maximum norm. Then we expect*

$$\|err\|_\infty \leq e^{\lambda N}, \tag{96}$$

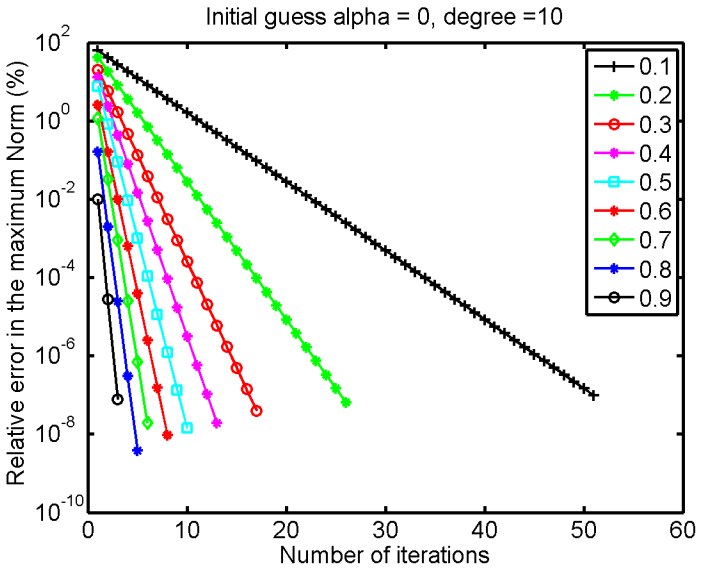

Figure 23: Relative error in the maximum norm(%) of numerical solutions of second order equation with smooth solution $u(x) = x^2 - x^3$

where λ is the rate of convergence.

Therefore,

$$\log \|Err_1\|_\infty \leq \lambda N_1,$$

$$\log \|Err_2\|_\infty \leq \lambda N_2,$$

$$\log \|\frac{Err_2}{Err_1}\|_\infty \approx \lambda(N_2 - N_1)$$

$$\lambda \approx \frac{\log \|\frac{Err_2}{Err_1}\|_\infty}{(N_2 - N_1)}$$

where N is the number of iterations. If the ratio of relative errors from Table 12 is plotted against the sizes of overlapping subdomains on xy-axis, then the convergence profile makes a quartic curve which is shown in Fig. 24 and is given by:

$$y = ax^4 + bx^3 + cx^2 + dx + e \tag{97}$$

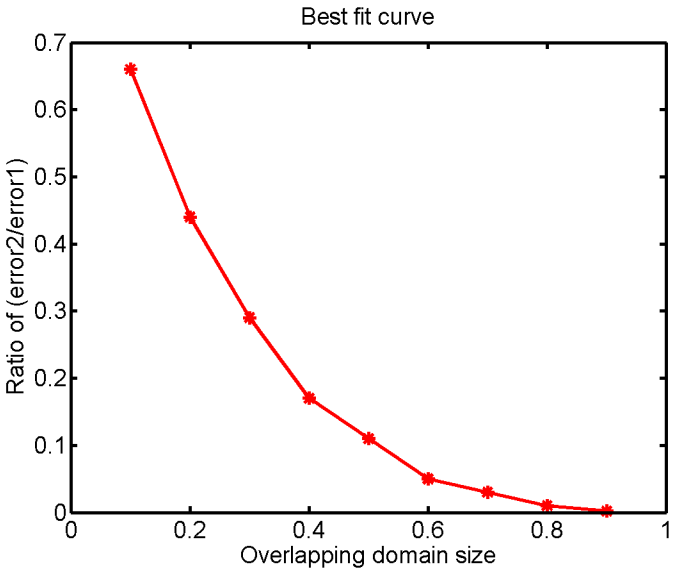

Figure 24: Ratio of relative errors in the maximum norm(%) versus sizes of overlapping subdomains for problem (94)

where

$$a = 1.63353,$$

$$b = -4.87451,$$

$$c = 6.05185,$$

$$d = -3.78608,$$

$$e = 0.990304.$$

Problem(94) is solved with respect to the following three combinations:

[I] IGA-Galerkin on Ω_1 and IGA-Galerkin on Ω_2

[II] IGA-Galerkin on Ω_1 and IGA-Collocation on Ω_2

[III] IGA-Collocation on Ω_1 and IGA-Collocation on Ω_2

Table 13: CPU time comparison for IGA-Galerkin and IGA-Galerkin, IGA-Galerkin and IGA-Collocation and IGA-Collocation and IGA-Collocation iterative methods

Iterative Method	CPU time(in seconds)
IGA-Galerkin and IGA-Galerkin	15.864
IGA-Galerkin and IGA-Collocation	7.175
IGA-Collocation and IGA-Collocation	0.6069

Consider the B-spline basis functions corresponding to following open knot vector,

$$U = \{\underbrace{0, ..., 0}_{10}, 0.1, 0.2, 0.3, 0.4, 0.5, 0.6, 0.7, 0.8, 0.9, \underbrace{1, ..., 1}_{10}\}.$$

Now the domain $[0, 1]$ is subdivided into two overlapping subdomains [0, 0.6] and [0.4, 1]. All three combinations yield the same results and require a count of 26 iterations to reach a solution of accuracy equal to 10^{-08} but the computing time for IGA-Collocation and IGA-Collocation combination is substantially less compared with the other two combinations. In other words, IGA-Collocation and IGA-Collocation combination is the most cost efficient method. Computing time for all three combinations is listed in Table 13.

5.3.2 One-dimensional Problem with Monotone Singularity

Consider the following second order elliptic equation:

$$\begin{cases} -u''(x) = f \qquad \text{for} \quad x \in (0, 1), \\ u(0) = u(1) = 0, \end{cases} \tag{98}$$

with the exact solution

$$u(x) = x^{\alpha} - x, \tag{99}$$

Table 14: Comparing relative errors in the maximum norm(%) for numercial solutions of Poisson equation, when true soltuion is $u(x) = x^\alpha - x$, with the intensity of singularity $\alpha = 0.65$

p-degree	DOF	without mapping	with mapping
$p = 5$	21	0.085	0.003
$p = 6$	25	0.041	0.0009
$p = 7$	29	0.014	0.0007
$p = 8$	33	0.006	0.00056
$p = 9$	37	0.004	0.00054
$p = 10$	41	0.003	0.000064

containing a monotone singularity with intensity $\alpha = 0.65$. To solve this problem, domain [0,1] is subdivided into overlapping subdomains $\Omega_1 = [0, \frac{3}{5}]$ and $\Omega_2 = [\frac{2}{5}, 1]$ with artificial boundaries $\Gamma_1 = \frac{3}{5}$ and $\Gamma_2 = \frac{2}{5}$. To apply the Schwarz alternating method, the initial guess on the artificial boundary Γ_1 is chosen to be 0. IGA-Galerkin method is used to solve subproblem (90) whereas IGA-Collocation method is used to solve subproblem (91). Subproblem(90) is solved in two different ways:

1- With using mapping techniques to solve subproblem(90) on subdomain Ω_1

2- Without using mapping techniques to solve subproblem(90) on subdomain Ω_1

For Ω_1, the subdomain of Ω which contains the singularity of u, the auxiliary mapping[16] $\varphi^\beta : \widehat{\Omega}_1 \longrightarrow \Omega_1$ is defined by:

$$\varphi^\beta(\xi) = (\xi)^\beta, \tag{100}$$

where ξ denotes the coordinate of the points in the transformed domain $\widehat{\Omega}_1$. Here β is called the **mapping size** of the auxiliary mapping. In this problem for $u(x) = x^\alpha - x$, where $\alpha = 0.65$. $u \circ \varphi^\beta = (\xi)^{\alpha\beta}$ is much smoother than x^α. In particular, if $\beta = 1/\alpha$, then $u \circ \varphi^\beta$ is smooth. Integrals in bilinear form are computed as discussed in remark-

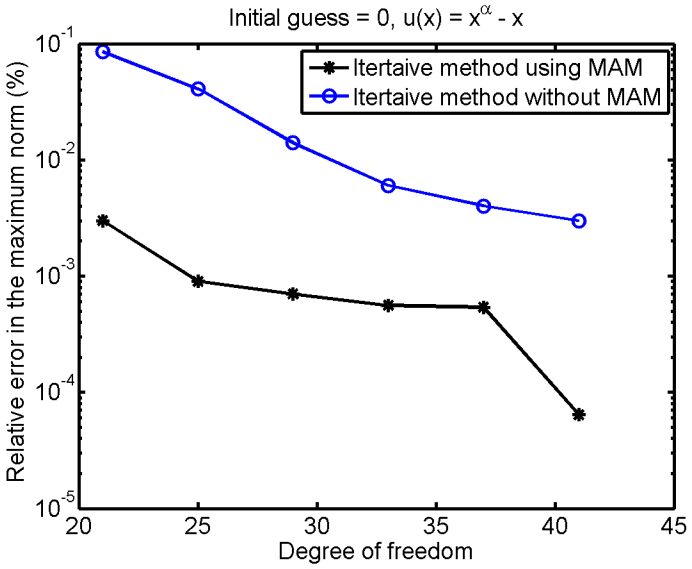

Figure 25: Relative error in the maximum norm(%) of numerical solutions of one-dimensional second order equation with nonregular solution $u(x) = x^{\alpha} - x$, when the intensity of singularity is $\alpha = 0.65$

2.1 of [16]. Table 14 and Fig. 25 show relative errors in the maximum norm(%) with respect to these two methods. The degree of the B-spline basis functions in subdomain Ω_2 is kept fixed while degree of the B-spline basis functions in subdomain Ω_1 is elevated.

5.4 Two-dimensional Problems

The Schwarz alternating method in the framework of IGA-Collocation is tested to two-dimensional problems in rectangular and circular domains. Performance of the method is checked for problems with both nonsingular and singular solutions.

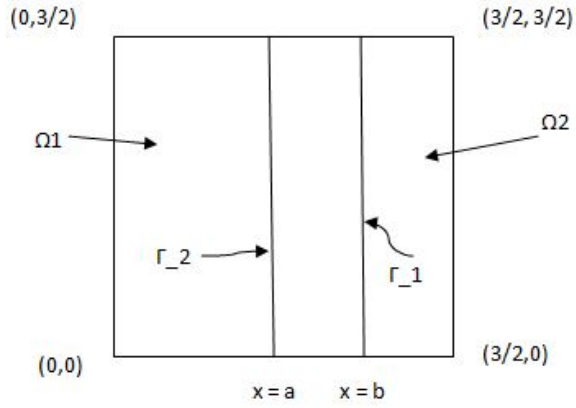

Figure 26: Rectangular subdomains $\Omega_1 = [0, b] \times [0, \frac{3}{2}]$ and $\Omega_2 = [a, 1] \times [0, \frac{3}{2}]$

5.4.1 The Poisson Equation on a Rectangular Domain

Model problem is an elliptic boundary value problem on the rectangle $\Omega = \left[0, \frac{3}{2}\right] \times \left[0, \frac{3}{2}\right]$

$$\begin{cases} -\Delta u = f \quad \text{for} \quad \Omega \\ u = 0 \quad \text{on} \quad \partial\Omega \end{cases} \tag{101}$$

with the exact solution:

$$u(x, y) = x^2 y^2 \left(x - \frac{3}{2}\right) \left(y - \frac{3}{2}\right). \tag{102}$$

Domain $\Omega = \left[0, \frac{3}{2}\right] \times \left[0, \frac{3}{2}\right]$ is divided into two overlapping subdomains Ω_1 and Ω_2 as shown in Fig. 26, with two artificial boundaries Γ_1 and Γ_2 such that $\Omega = \Omega_1 \cup \Omega_2$ where $\Omega_1 = [0, \Gamma_1] \times [0, \frac{3}{2}]$ and $\Omega_2 = [\Gamma_2, \frac{3}{2}] \times [0, \frac{3}{2}]$. Here, $\Gamma_2 = a$ and $\Gamma_1 = b$. Mappings F_1 and F_2 are smooth linear mappings which map the reference space $\widehat{\Omega}$ onto the physical spaces Ω_1 and Ω_2, respectively and are further defined in the following way:

$F_1 : \hat{\Omega} \to \Omega_1$ and $F_1(u,v) = (x(u,v), y(u,v))$ such that,

$$F_1(u,v) = \begin{cases} x(u,v) = bu \\ y(u,v) = \frac{3}{2}v. \end{cases} \tag{103}$$

$F_2 : \hat{\Omega} \to \Omega_2$ and $F_2(u,v) = (x(u,v), y(u,v))$ is defined by

$$F_2(u,v) = \begin{cases} x(u,v) = (1.5-a)u + a \\ y(u,v) = \frac{3}{2}v. \end{cases} \tag{104}$$

The following subproblem is first solved using IGA-Collocation method in the subdomain Ω_1 with an initial guess $u_2^0(x,y) = 0$ on the artificial boundary Γ_1 and zero boundary condition on the boundary $\Omega_1 \setminus \Gamma_1$

$$\begin{cases} -\Delta u_1^{n+1} = f \quad \text{for} \quad \Omega_1 \\ u_1^{n+1}(x,y) = 0 \quad \text{on} \quad \partial\Omega_1 \setminus \Gamma_1 \\ u_1^{n+1}(x,y) = u_2^n(x,y) \quad \text{on} \quad \Gamma_1 \end{cases} \tag{105}$$

and then the following subproblem in subdomain Ω_2 is solved. This iterative process is terminated when it reaches either a count of 50 iterations or the solution of desired accuracy of $\| err \|_\infty \leq 10^{-12}$ is obtained, whichever comes first.

$$\begin{cases} -\Delta u_2^{n+1} = f \quad \text{for} \quad \Omega_2 \\ u_2^{n+1}(x,y) = 0 \quad \text{on} \quad \partial\Omega_2 \setminus \Gamma_2 \\ u_2^{n+1}(x,y) = u_1^{n+1}(x,y) \quad \text{on} \quad \Gamma_2 \end{cases} \tag{106}$$

This problem is tested for various overlapping sizes. Like in the one-dimension case, the number of iterations required to get the solution of accuracy $\| err \|_\infty \leq 10^{-12}$ is dependent upon the size of the overlapping region but not on the location of artificial

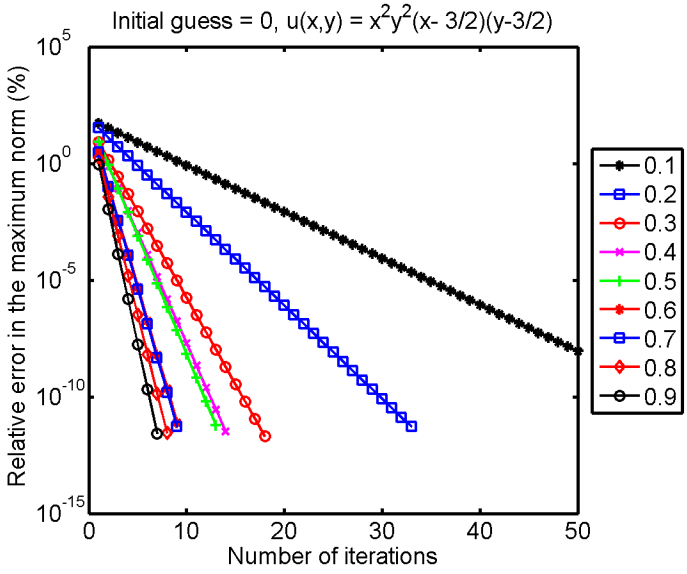

Figure 27: Relative error in the maximum norm(%) for Problem(101) with true solution $u(x) = x^2y^2(x - \frac{3}{2})(y - \frac{3}{2})$

Table 15: Size of overlapping region and the number of iterations required to get a solution of accuracy 10^{-12}

Overlapping Size	0.1	0.2	0.3	0.4	0.5	0.6	0.7	0.8	0.9
Iterations	50	33	18	14	13	9	9	8	7

boundaries. Relative errors in the maximum norm in (%) for different overlapping sizes are shown in Table 15 and Fig. 27.

5.4.2 Two-dimensional Elliptic Equations Containing Singularities

The problem discussed here has a crack singularity of type $r^{1/2}$ on a circular domain of radius 2 and centered at origin. This circular domain is decomposed into a circle $\Omega_1 = [(r, \theta) : r < r_1, 0 < \theta < 2\pi]$ and a annulus $\Omega_2 = [(r, \theta) : r_2 < r < 2, 0 < \theta < 2\pi]$ as shown in Fig. 28. Consider the following Poisson equation:

$$\begin{cases} -\Delta u = f \quad \text{in} \quad \Omega \\ u = 0 \quad \text{on} \quad \partial\Omega \end{cases} \tag{107}$$

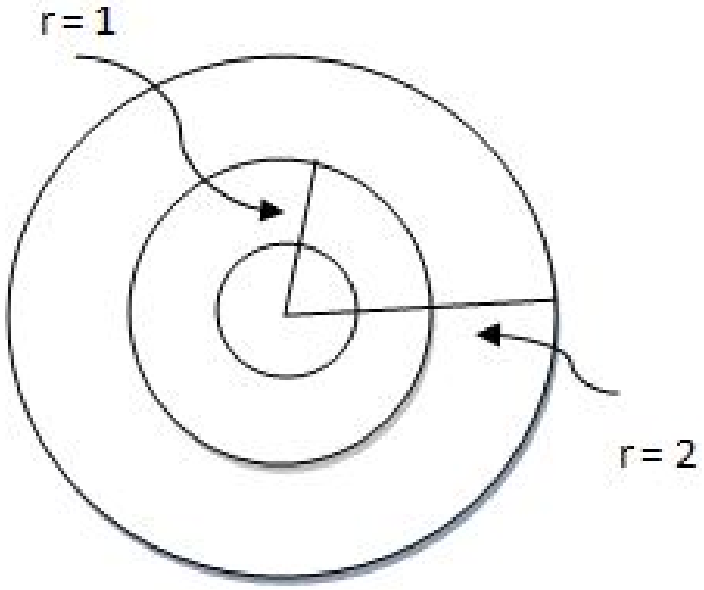

Figure 28: Circular subdomain $\Omega_1 = [(r,\theta) : r \leq 1, 0 < \theta < 2\pi]$ and annular subdomain $\Omega_2 = [(r,\theta) : 0.5 \leq r \leq 2, 0 < \theta < 2\pi]$

with the exact solution:

$$u(r,\theta) = \sqrt{r}(1-r)\left[\sin\left(\frac{\theta}{2}\right) + \sin\left(\frac{3\theta}{2}\right)\right]. \tag{108}$$

Smooth mapping F_1 maps the reference domain $\hat{\Omega}$ onto the physical subdomain Ω_1,

$$F_1 : \hat{\Omega} = [0,1] \times [0,1] \longrightarrow \Omega_1 = \{(x,y) : 0 \leq x^2 + y^2 \leq r_1^2\},$$

$$F_1(u,v) = \begin{cases} x(u,v) = r_1 v^2 \cos(2\pi(1-u)) \\ \\ y(u,v) = r_1 v^2 \sin(2\pi(1-u)). \end{cases} \tag{109}$$

Mapping F_2 maps the reference domain $\hat{\Omega}$ onto the physical subdomain Ω_2,

$$F_2 : \hat{\Omega} = [0,1] \times [0,1] \longrightarrow \Omega_2 = \{(x,y) : r_2^2 \leq x^2 + y^2 \leq 2\},$$

$$F_2(u,v) = \begin{cases} x(u,v) = r_2(1-v)\cos(2\pi(1-u)) + 2v\cos(2\pi(1-u)) \\ y(u,v) = r_2(1-v)\sin(2\pi(1-u)) + 2v\sin(2\pi(1-u)). \end{cases} \tag{110}$$

where r_1 is the radius of singular subdomain and r_2 is the radius of inner circle of annulus. Accuracy of the solution depends on the choice of r_1 and r_2. Since this is the problem with crack singularity of type $r^{\frac{1}{2}}$, the initial guess is chosen $u_2^0 = \sqrt{r}\sin(\theta/2)$ along the artificial boundary Γ_1 of subdomain Ω_1 to solve the following subproblem,

$$\begin{cases} -\Delta u_1^{n+1} = f \quad \text{in} \quad \Omega_1 \\ u_1^{n+1} = u_2^n \quad \text{on} \quad \Gamma_1 \\ u_1^{n+1} = 0 \quad \text{on} \quad \partial\Omega_1 \cap \partial\Omega. \end{cases} \tag{111}$$

Once the solution for this subproblem is found, then the below problem is solved in subdomain Ω_2.

$$\begin{cases} -\Delta u_2^{n+1} = f \quad \text{in} \quad \Omega_2 \\ u_2^{n+1} = u_1^{n+1} \quad \text{on} \quad \Gamma_2 \\ u_2^{n+1} = 0 \quad \partial\Omega_2 \cap \partial\Omega. \end{cases} \tag{112}$$

In the non-singular case, the number of iterations required to reach the solution of desired accuracy is dependent upon the values of radius r_2 and r_1 as well as the size of the overlapping domain. If r_1, the radius of circular subdomain with singularity, is very small, then it takes more iterations to converge. Relative errors in the maximum norm (%) are displayed in Fig. 29.

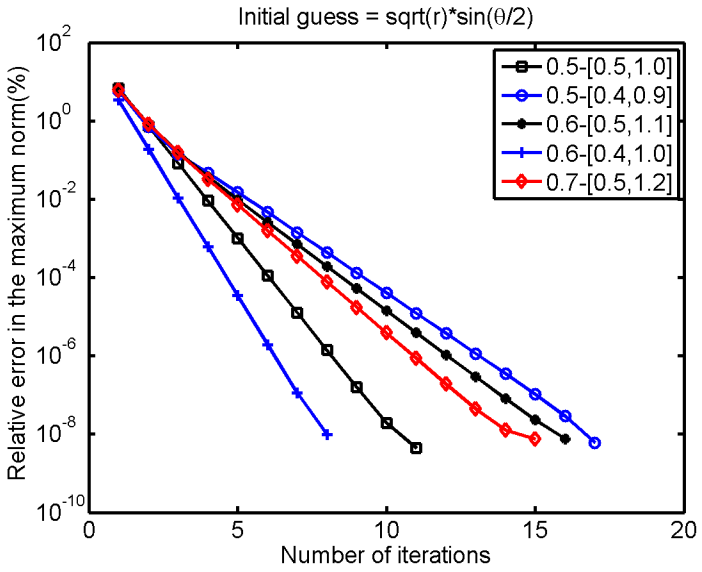

Figure 29: Relative errors in the maximum norm(%) for various overlapping sizes for crack singularity problem on a circular domain whose true solution is given by $u(r,\theta) = \sqrt{r}(1-r)\left[\sin\left(\frac{\theta}{2}\right) + \sin\left(\frac{3\theta}{2}\right)\right]$

CHAPTER 6: ALTERNATING METHOD FOR TWO NON-OVERLAPPING SUBDOMAINS

The previous chapter explained using the Schwarz alternating method in the framework of IGA-Collocation when the domain is subdivided into two overlapping subdomains. This chapter will focus on how to impose the same method when the domain is subdivided into two non-overlapping subdomains. In non-overlapping methods, the subdomains intersect only on their interface.

Consider the Poisson problem

$$\begin{cases} -\Delta u = f \quad \text{in} \quad \Omega, \\ u = 0 \quad \text{on} \quad \partial\Omega, \end{cases} \tag{113}$$

on a bounded Lipschitz region Ω with homogeneous boundary condition on boundary $\partial\Omega$. Domain Ω is divided into two non-overlapping subdomains Ω_1 and Ω_2 with common internal boundary Γ. Like in the overlapping subdomain problem, this problem will also be solved by solving two subproblems. These subproblems can be solved in two different ways by imposing two different boundary conditions on the interface [21]:

1. The Dirichlet-Neumann method

2. The Neumann-Neumann method

6.1 The Dirichlet-Neumann Method

In this method for given initial guess λ^0, problem(113) will be split into the following two subproblems. For each $k \geq 0$:

$$\begin{cases} -\Delta u_1^{k+1} = f \quad \text{in} \quad \Omega_1, \\ u_1^{k+1} = 0 \quad \text{on} \quad \partial\Omega_1 \cap \partial\Omega, \\ u_1^{k+1} = \lambda^k \quad \text{on} \quad \Gamma. \end{cases} \tag{114}$$

and

$$\begin{cases} -\Delta u_2^{k+1} = f \quad \text{in} \quad \Omega_2, \\ u_2^{k+1} = 0 \quad \text{on} \quad \partial\Omega_2 \cap \partial\Omega, \\ \dfrac{\partial u_2^{k+1}}{\partial n} = \dfrac{\partial u_1^{k+1}}{\partial n} \quad \text{on} \quad \Gamma. \end{cases} \tag{115}$$

with

$$\lambda^{k+1} := \theta u_{2|\Gamma}^{k+1} + (1-\theta)\lambda^k, \tag{116}$$

where $\theta, 0 \leq \theta \leq 1$ is a positive accelerated parameter.

A similar alternating procedure can be obtained if the subproblems are changed in the following manner:

$$\begin{cases} -\Delta u_1^{k+1} = f \quad \text{in} \quad \Omega_1, \\ u_1^{k+1} = 0 \quad \text{on} \quad \partial\Omega_1 \cap \partial\Omega, \\ u_1^{k+1} = u_2^k \quad \text{on} \quad \Gamma. \end{cases} \tag{117}$$

and

$$\begin{cases} -\Delta u_2^{k+1} = f \quad \text{in} \quad \Omega_2, \\ u_2^{k+1} = 0 \quad \text{on} \quad \partial\Omega_2 \cap \partial\Omega, \\ \dfrac{\partial u_2^{k+1}}{\partial n} = \mu^k \quad \text{on} \quad \Gamma. \end{cases} \tag{118}$$

with

$$\mu^{k+1} := \theta \frac{\partial u_1^{k+1}}{\partial n} + (1-\theta)\mu^k. \tag{119}$$

6.2 The Neumann-Neumann Method

In this case, for eack $k \geq 0$ we need to solve:

$$\begin{cases} -\Delta u_i^{k+1} = f \quad \text{in} \quad \Omega_i, \\ u_i^{k+1} = 0 \quad \text{on} \quad \partial\Omega_i \cap \partial\Omega, \\ u_i^{k+1} = \lambda^k \quad \text{on} \quad \Gamma, \end{cases} \tag{120}$$

and then solve

$$\begin{cases} -\Delta v_i^{k+1} = 0 \quad \text{in} \quad \Omega_i, \\ v_i^{k+1} = 0 \quad \text{on} \quad \partial\Omega_i \cap \partial\Omega, \\ \dfrac{\partial v_i^{k+1}}{\partial n} = \dfrac{\partial u_1^{k+1}}{\partial n} - \dfrac{\partial u_2^{k+1}}{\partial n} \quad \text{on} \quad \Gamma, \end{cases} \tag{121}$$

for $i = 1, 2$, with

$$\lambda^{k+1} := \lambda^k - \theta \left\{ a_1 v_{1|\Gamma}^{k+1} - a_2 v_{2|\Gamma}^{k+1} \right\}. \tag{122}$$

As before, θ is a positive accelerated parameter, a_1 and a_2 are two positive averaging coefficients, where λ^0 is the initial guess.

6.3 Numerical Examples

For numerical computations, examples in this section are solved by splitting rectangular domain into two non-overlapping subdomains in two different ways:

- Division by a vertical interface
- Division by a slanted interface

as shown in Fig. 30. This dissertation focuses on obtaining solution of the problems by solving Dirichlet-Neumann subproblems(114)-(115) in two non-overlapping subdomains.

6.3.1 Vertical Interface in a Rectangular Domain

Consider a two-dimensional elliptic boundary value problem with a vertical subdivision of domain $\Omega = [-1, 1] \times [0, 1]$

$$\begin{cases} -\Delta u = f \quad \text{for} \quad \Omega \\ u = 0 \quad \text{on} \quad \partial\Omega \end{cases} \tag{123}$$

with the exact solution:

$$u(x, y) = e^x(1 - x^2)(y - y^2). \tag{124}$$

To solve problem (123), the domain $\Omega = [-1, 1] \times [0, 1]$ is divided into two non-overlapping subdomains $\Omega_1 = [-1, 0] \times [0, 1]$ and $\Omega_2 = [0, 1] \times [0, 1]$ with common interface at $\Gamma = a$. For this vertical subdivision, two linear mappings, F_1 and F_2 are used to map the parameter domain onto subdomains Ω_1 and Ω_2 with common internal boundary Γ at $a = 0$. $F_1 : \hat{\Omega} \to \Omega_1$ and $F_1(u, v) = (x(u, v), y(u, v))$ is defined

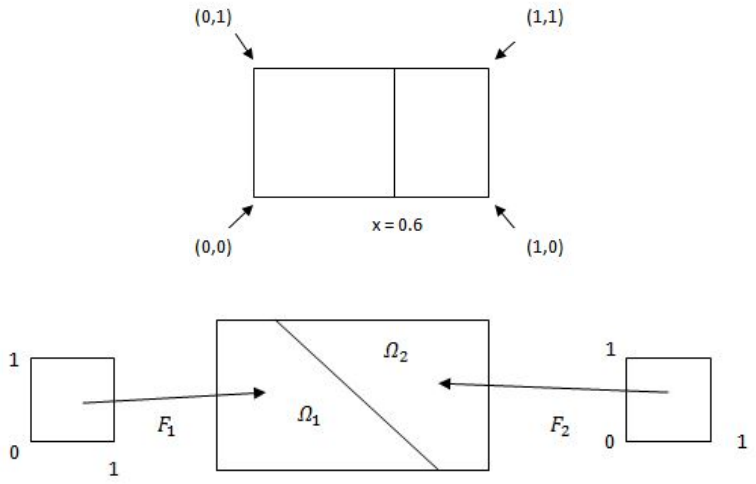

Figure 30: (a) Division by a vertical interface (b) Division by a slanted interface

by

$$F_1(u,v) = \begin{cases} x(u,v) = (a+1)u - 1 \\ y(u,v) = v. \end{cases} \tag{125}$$

$F_2 : \hat{\Omega} \to \Omega_2$ and $F_2(u,v) = (x(u,v), y(u,v))$ is defined by

$$F_2(u,v) = \begin{cases} x(u,v) = (1-a)u + a \\ y(u,v) = v. \end{cases} \tag{126}$$

In order to solve problem(123), subproblems(114) and (115) are solved by assuming an initial guess $\lambda^0 = 0.5$. For the subdomain Ω_2, separate equations are needed for those collocation points that lie on the interface Γ. No additional equations are needed for collocation points that lie on the homogeneous boundary. For points p_i that lie inside the domain, the following equation is used:

$$(-\Delta u)(p_i) = f(p_i). \tag{127}$$

For points that lie on Neumann boundary subdomain Ω_2, the following equation is

Table 16: Comparison of relative error in the maximum norm in(%) for nonoverlapping domain problem for different θ values

Iteration	$\theta = 0.4$	$\theta = 0.5$	$\theta = 0.6$
1	3.192E+01	1.94E+00	3.192E+01
2	6.38E+00	1.32E-01	6.38E+00
3	1.27E+00	8.20E-03	1.27E+00
4	2.55E-01	5.09E-04	2.55E-01
5	5.11E-02	3.16E-05	5.11E-02
6	1.02E-02	1.96E-06	1.02E-02
7	2.04E-03	1.22E-07	2.04E-03
8	4.09E-04	7.52E-09	6.60E-04
9	8.17E-05	4.93E-10	2.14E-04
10	1.63E-05	5.26E-11	6.52E-05
11	3.27E-06	-	1.92E-05
12	6.54E-07	-	5.54E-06
13	1.31E-07	-	1.57E-06
14	2.61E-08	-	4.43E-07
15	5.23E-09	-	1.24E-07
16	1.05E-09	-	3.44E-08
17	2.25E-10	-	9.55E-09
18	8.62E-11	-	2.61E-09
19	-	-	7.51E-10
20	-	-	1.80E-10
21	-	-	8.98E-11

used:

$$\frac{\partial u_2^{k+1}}{\partial n}(p_i) = \frac{\partial u_1^{k+1}}{\partial n}(p_i). \tag{128}$$

The non-overlapping alternating method is tested with respect to various relaxation parameters θ. The relative errors in the maximum norm(%) for these parameters are shown in Table 16 and Fig. 31. It required only 10 iterations for $\theta = 0.5$ where as for $\theta = 0.4$ and for $\theta = 0.6$ it required more number of iterations to converge. Therefore the optimal value of θ is considered to be $\theta = 0.5$ for this problem with subdivision at $x = 0$.

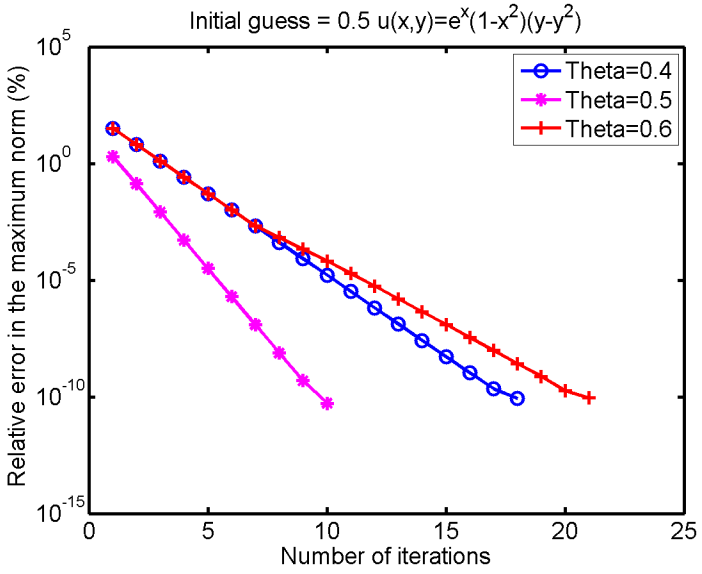

Figure 31: Relative erros in the maximum norm(%) for various values of parameter θ when domain is divided into two nonoverlapping subdomains

6.3.2 Slanted Interface in a Rectangular Domain

The following problem is tested with a slanted subdivision at the interface on the domain $\Omega = [-1, 1] \times [0, 1]$

$$\begin{cases} -\Delta u = f \quad \text{for} \quad \Omega \\ u = 0 \quad \text{on} \quad \partial\Omega \end{cases} \tag{129}$$

with the exact solution:

$$u(x, y) = x^3(1 - x^2)(y - y^2). \tag{130}$$

For this subdivision nonlinear mappings F_1 and F_2 are used to map the reference domain $\widehat{\Omega} = [0, 1] \times [0, 1]$ to the physical subdomains Ω_1 and Ω_2, respectively.

$$F_1(u, v) = (0, 0)\, L_1(u, v) + \left(\frac{1}{2}, 0\right) L_2(u, v) + \left(-\frac{1}{2}, 1\right) L_3(u, v) + (0, 1)\, L_4(u, v) \tag{131}$$

$$F_2(u, v) = \left(\frac{1}{2}, 0\right) L_1(u, v) + (1, 0)\, L_2(u, v) + (1, 1)\, L_3(u, v) + \left(-\frac{1}{2}, 1\right) L_4(u, v) \tag{132}$$

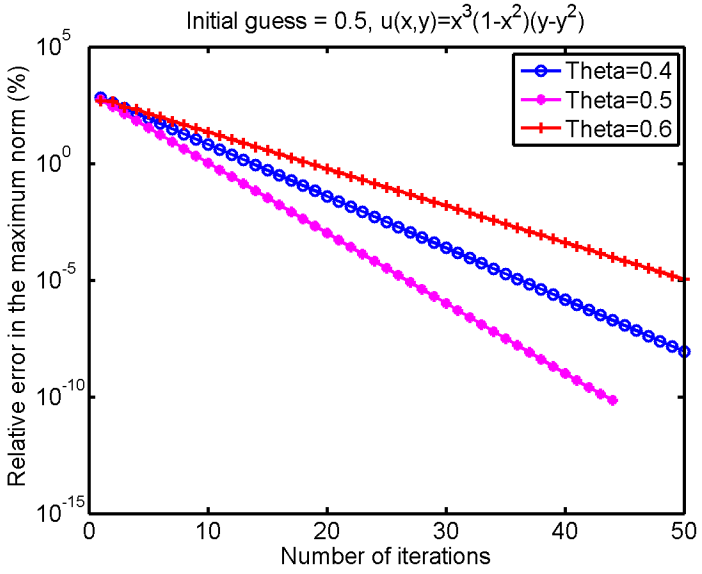

Figure 32: Relative error in the maximum norm(%) for problem with slanted nonoverlapping subdomains

where,

$$L_1(u,v) = (1-u)(1-v), \quad L_2(u,v) = u(1-v),$$
$$L_3(u,v) = uv, \quad L_4(u,v) = (1-u)v. \tag{133}$$

Like the vertical division problem, this problem is solved by solving subproblems(114) and (115) in the framework of IGA-Collocation and by assuming initial guess $\lambda^0 = 0.5$. The non-overlapping alternating method with slanted subdivision is tested with respect to various relaxation parameters θ. The results are shown in Fig. 32. Like in the vertical division case, $\theta = 0.5$ is the optimal value and it took 44 iterations to get the solution with accuracy 10^{-11}.

CHAPTER 7: ALTERNATING METHOD IN IGA COLLOCATION FOR ELASTICITY PROBLEMS

In Chapter 5, an alternating method in the framework of IGA-Collocation is presented for one and two dimensional elliptic boundary value problems. In this chapter, this method is extended to linear elasticity, where coupled elliptic equations are involved in order to solve the problem.

7.1 Preliminaries

This section presents the notations, terminologies and definitions related to linear elasticity. For any displacement vector $\{u\} = \{u_1(x,y), u_2(x,y)\}^T$, the stress field is defined by $\{\sigma\} = \{\sigma_x, \sigma_y, \tau_{xy}\}^T$ and the strain field is defined by $\{\varepsilon\} = \{\varepsilon_x, \varepsilon_y, \gamma_{xy}\}^T$.$\sigma_x$ and σ_y are normal stress and τ_{xy} is shear stress. Similarly, ε_x and ε_y are normal strain and γ_{xy} is shear strain. The relation between strain-displacement and stress-strain is given by

$$\{\varepsilon\} = [D]\{u\}, \quad \{\sigma\} = [E]\{\varepsilon\}, \tag{134}$$

where $[D]$ is the differential operator matrix and $[E]$ is the material stiffness matrix given by 3×3 symmetric positive definite matrix of material constants. Matrix $[D]$

is given by

$$[D] = \begin{pmatrix} \dfrac{\partial}{\partial x} & 0 \\ 0 & \dfrac{\partial}{\partial y} \\ \dfrac{\partial}{\partial y} & \dfrac{\partial}{\partial x} \end{pmatrix}. \tag{135}$$

Generally there are two types of problems that are involved in linear elasticity, *plain stress* and *plain strain*. Plane stress is defined to be a state of stress in which normal stress σ_z and shear stresses τ_{xz} and τ_{yz} are assumed to be zero. Plane strain is defined to be a state of strain in which normal strain ε_z and shear strains γ_{xz} and γ_{yz} are assumed to be zero.

Materials that have identical values for properties in all directions are called Isotropic materials. These materials have two components, Young's modulus(E) and Poisson's ration(ν). The range of Poisson's ratio is $0 \leq \nu \leq 0.5$. The material stiffness matrix $[E]$ for an isotropic elastic body is as follows:

$$[E] = \frac{E}{1-\nu^2} \begin{pmatrix} 1 & \nu & 0 \\ \nu & 1 & 0 \\ 0 & 0 & \frac{1-\nu}{2} \end{pmatrix} \quad \text{for plane stress,} \tag{136}$$

$$[E] = \begin{pmatrix} \zeta + 2\mu & \zeta & 0 \\ \zeta & \zeta + 2\mu & 0 \\ 0 & 0 & \mu \end{pmatrix} \quad \text{for plane strain,} \tag{137}$$

where

$$\mu = \frac{E}{2(1+\nu)}, \quad \zeta = \frac{\nu E}{(1+\nu)(1-2\nu)} \tag{138}$$

The equilibrium equation of elasticity is

$$[D]^T\{\sigma\}(x,y) + \{f\}(x,y) = 0, \quad (x,y) \in \Omega, \tag{139}$$

where $\{f\} = \{f_1(x,y), f_2(x,y)\}^T$ is the vector of internal sources representing the body force per unit area. This equilibrium equation can be written in terms of displacement in the following way,

$$\{\sigma\} = [E]\{\varepsilon\},$$

$$\{\sigma\} = [E][D]\{u\},$$

$$\{\sigma\} = \frac{E}{1-\nu^2}\begin{pmatrix} 1 & \nu & 0 \\ \nu & 1 & 0 \\ 0 & 0 & \frac{1-\nu}{2} \end{pmatrix}\begin{pmatrix} \frac{\partial}{\partial x} & 0 \\ 0 & \frac{\partial}{\partial y} \\ \frac{\partial}{\partial y} & \frac{\partial}{\partial x} \end{pmatrix}\begin{pmatrix} u_1(x,y) \\ u_2(x,y) \end{pmatrix}.$$

The Navier equations for plane stress are

$$\frac{E}{1-\nu^2}\left[\frac{\partial^2 u_1}{\partial x^2} + \frac{(1+\nu)}{2}\frac{\partial^2 u_2}{\partial x \partial y} + \frac{(1-\nu)}{2}\frac{\partial^2 u_1}{\partial y^2}\right] + f_1(x,y) = 0 \tag{140}$$

$$\frac{E}{1-\nu^2}\left[\frac{(1-\nu)}{2}\frac{\partial^2 u_2}{\partial y^2} + \frac{(1+\nu)}{2}\frac{\partial^2 u_1}{\partial x \partial y} + \frac{\partial^2 u_2}{\partial y^2}\right] + f_2(x,y) = 0. \tag{141}$$

Similarly, the Navier equations for plane strain are

$$(\zeta + 2\mu)\frac{\partial^2 u_1}{\partial x^2} + (\zeta + \mu)\frac{\partial^2 u_2}{\partial x \partial y} + \mu\frac{\partial^2 u_1}{\partial y^2} + f_1(x,y) = 0 \tag{142}$$

$$\mu\frac{\partial^2 u_2}{\partial y^2} + (\zeta+\mu)\frac{\partial^2 u_1}{\partial x \partial y} + (\zeta+2\mu)\frac{\partial^2 u_2}{\partial y^2} + f_2(x,y) = 0. \tag{143}$$

Three dimensional elasticity problems are complex to solve, thus different methods are used to reduce the dimension in different ways such as planar, axisymmetric, shell, plate beam and bar models. When assuming $u_z = 0$, $\sigma_z = \tau_{yz} = \tau_{zx} = 0$ in plane stress and in the case of plane strain $\epsilon_z = \gamma_{yz} = \gamma_{zx} = 0$.

7.2 Alternating Method for Elasticity Problems

To solve Navier's equation either in the plane stress or in the plane strain case, the components of the displacement vector are written in terms of basis functions, $\phi_i(x,y), i = 1, ..., N$,

$$\{u(x,y)\} = \begin{cases} u_1(x,y) = \sum_{i=1}^{N} c_i \phi_i(x,y), \\ u_2(x,y) = \sum_{i=1}^{N} c_{i+N} \phi_i(x,y) \end{cases} \tag{144}$$

where $c_i (i = 1, 2, ..., 2N)$ are called the amplitudes of the basis functions and $\phi_i(x,y) = (N_r(u) \times M_s(v)) \circ G^{-1}$, is the tensor product of B-spline basis functions $N_r(u)$ and $M_s(v)$ in the u- and v-direction, respectively and $G : [0,1]\times[0,1] \longrightarrow \Omega$ is a geometric map. Collocation points $p_i = G(u_i, v_i)$ are chosen using the tensor-product of *Greville abscissae* defined in chapter 3. Collocation equations for (139) are given by

$$[D]^T\{\sigma\}(p_i) + \{f\}(p_i) = 0, \quad \text{for} \quad \text{collocation points} \quad p_i, i = 1, 2, ..., N. \tag{145}$$

Thus dividing a domain into two overlapping subdomains and solving (145) in each subdomain and continuously updating the solutions at interior boundaries like it is done in chapter 5, will yield the solution of the elasticity problem.

7.3 Numerical Examples

This alternating method is tested for both singular and nonsingular problems in two dimensions. The non-singular problem is tested on a rectangular domain whereas the singular problem is tested on a wedge shaped domain with singularity of intensity $\lambda = 0.5$. Plane stress Navier's equations are used for nonsingular case and plane strain Navier's equations are used for singular case.

7.3.1 Non-singular Two-dimensional Problem on Rectangular Domain

This problem is tested on domain $\Omega = [0,1] \times [0,1]$ and the isotropic material is assumed to have material constant $E = 1000$ and $\nu = 0.3$.

$$\begin{cases} [D]^T\{\sigma\}(x,y) + \{f\}(x,y) = 0, \quad (x,y)\epsilon\Omega \\ u_1(x,y) = 0, \quad u_2(x,y) = 0, \quad \text{on} \quad \partial\Omega. \end{cases} \tag{146}$$

with manufactured exact solution:

$$\{u(x,y)\} = \begin{cases} u_1(x,y) = x(1-x)y^3(1-y), \\ u_2(x,y) = y(1-y)x^3(1-x). \end{cases} \tag{147}$$

The alternating process started with 9 basis functions of degree 5 in u-direction and 4 basis functions of degree 3 in v-direction which gave us a total of 36 basis functions by taking their tensor products. For collocation points, Greville absciaase are used in both directions which gives a total of 36 collocation points by tensor product. Since there are two components in the Navier's equation so a total of $2(36) = 72$ collocation points are needed to solve the problem. Therefore these 36 points are used for both components. The size of the stiffness matrix is 72×72.

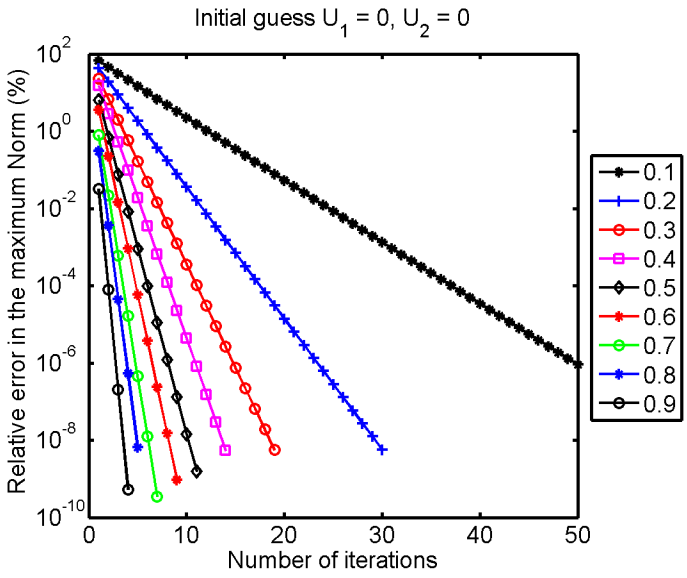

Figure 33: Relative error in the maximum norm in(%) for different overlapping domain sizes for nonsingular elasticity problem

The alternating scheme is repeated for two different overlapping domains with various sizes of overlapping regions. Like in one elliptic boundary value problem, the number of iterations required is dependent upon the size of the overlapping area. Fig. 33 shows that if overlapping area is larger, then it will require less number of iterations.

7.3.2 Two-dimensional Singular Problem on Wedge Shaped Domain

Consider a two dimensional coupled elliptic boundary value problem for a wedge shaped domain $\Omega^{(\pm\alpha)} = \{(r,\theta) : r < 2, -\alpha \leq \theta \leq \alpha\}$, $0 \leq \alpha \leq 90^\circ$ for plane strain case, where α is the wedge angle and the body force is neglected here. The isotropic material is assumed to have material constant $E = 1000$ and $\nu = 0.3$. For the numerical example, we choose the wedge angle to be $\alpha = 60^\circ$, then the resulting

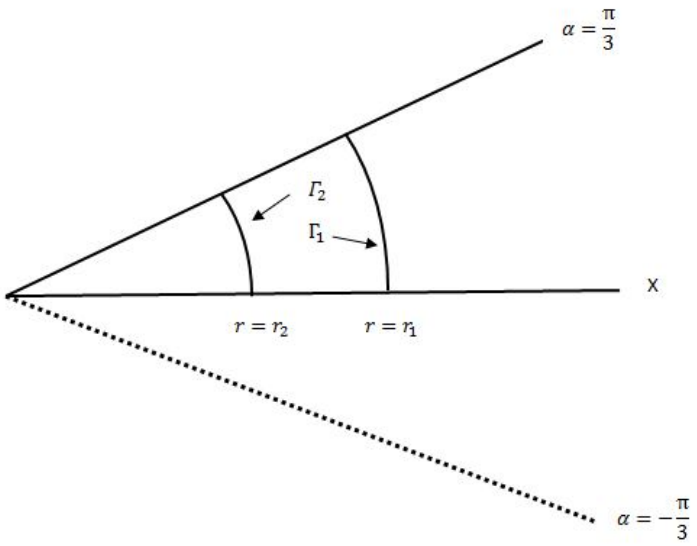

Figure 34: Wedge domain shape for elasticity problem containing singularities

singularity becomes as strong as the crack singularity.

$$[D]^T\{\sigma\}(x,y) + \{f\}(x,y) = 0, \quad (x,y) \in \Omega^{(\pm\alpha)}, \tag{148}$$

with the exact solution in the form:

$$\{u(x,y)\} = \begin{cases} u_1(x,y) = u_r \cos\theta - u_\theta \sin\theta, \\ \\ u_2(x,y) = u_r \cos\theta + u_\theta \sin\theta, \end{cases} \tag{149}$$

where

$$\begin{aligned} u_r(r,\theta) &= \tfrac{r^\lambda}{2G}\{-(\lambda+1)f(\theta)\} \\ u_\theta(r,\theta) &= \tfrac{r^\lambda}{2G}\{-f'(\theta)\}, \end{aligned} \tag{150}$$

and $f(\theta) = \sin(\lambda+1)\theta, \quad \lambda = \frac{90^\circ}{\alpha} - 1$. A non-homogeneous Dirichlet boundary condition is imposed along the entire boundary except at the origin where zero boundary condition is imposed for the displacement vector. Domain $\Omega^{(+\alpha)}$ is divided into two subdomains $\Omega_1^{(+\alpha)}$ and $\Omega_2^{(+\alpha)}$ as shown in Fig. 34. Smooth mapping F_1 maps the

Table 17: Number of iterations required to get solution of accuracy 10^{-7} for fixed value of r_1 with various overlapping domain sizes for elasticity problem containing singularities

Overlap Size	r_1	r_2	Number of iterations
0.6	1.0	0.4	8
0.5	1.0	0.5	10
0.4	1.0	0.6	13
0.3	1.0	0.7	19
0.2	1.0	0.8	30

reference domain Ω onto the physical subdomain $\Omega_1^{(+\alpha)}$,

$$F_1 : \hat{\Omega} = [0,1] \times [0,1] \longrightarrow \Omega_1^{(+\alpha)} = \{(x,y) : 0 \leq x^2 + y^2 \leq r_1^2, y \geq 0, \alpha = 60^\circ\}$$

$$F_1(u,v) = \begin{cases} x(u,v) = r_1 v^2 \cos\left(\dfrac{\pi\alpha u}{180^\circ}\right) \\ y(u,v) = r_1 v^2 \sin\left(\dfrac{\pi\alpha u}{180^\circ}\right). \end{cases} \tag{151}$$

Mapping F_2 maps the reference domain Ω onto the physical subdomain $\Omega_2^{(+\alpha)}$,

$$F_2 : \hat{\Omega} = [0,1] \times [0,1] \longrightarrow \Omega_2^{(+\alpha)} = \{(x,y) : r_2^2 \leq x^2 + y^2 \leq 2, y \geq 0, \alpha = 60^\circ\}$$

$$F_2(u,v) = \begin{cases} x(u,v) = r_2(1-v)\cos\left(\dfrac{\pi\alpha u}{180^\circ}\right) + 2v\cos\left(\dfrac{\pi\alpha u}{180^\circ}\right) \\ y(u,v) = r_2(1-v)\sin\left(\dfrac{\pi\alpha u}{180^\circ}\right) + 2v\sin\left(\dfrac{\pi\alpha u}{180^\circ}\right) \end{cases} \tag{152}$$

where r_1 is the radius of singular subdomain and r_2 is the radius of inner circle of regular subdomain. The accuracy of the solution depends on the choice of r_1 and r_2. Since this is the problem with singularity of type $r^{\frac{1}{2}}$, without loss of generality the initial guess can be chosen $u_1(r,\theta) = \sqrt{r}\sin(\frac{\theta}{2})$ and $u_2(r,\theta) = \sqrt{r}\cos(\frac{\theta}{2})$ along the artificial boundary Γ_1 of subdomain Ω_1

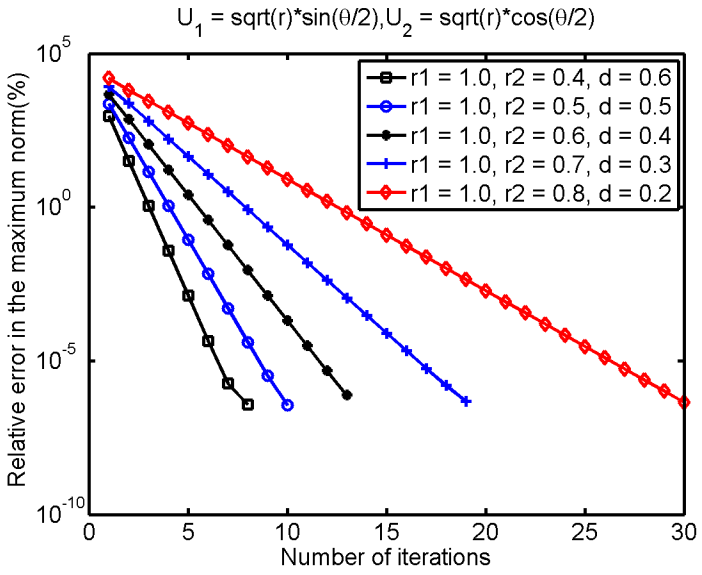

Figure 35: Relative error in the maximum norm in(%) for various overlapping sizes for elasticity problem containing singularities

It is not difficult to show that

$$\frac{\partial^2 u_1}{\partial x^2} = -\frac{\lambda(1+\lambda)(\lambda-1)}{2G} r^{\lambda-2} \sin(\lambda-2)\theta, \tag{153}$$

$$\frac{\partial^2 u_1}{\partial xy} = -\frac{\lambda(1+\lambda)(\lambda-1)}{2G} r^{\lambda-2} \cos(\lambda-2)\theta, \tag{154}$$

$$\frac{\partial^2 u_1}{\partial y^2} = +\frac{\lambda(1+\lambda)(\lambda-1)}{2G} r^{\lambda-2} \sin(\lambda-2)\theta, \tag{155}$$

$$\frac{\partial^2 u_2}{\partial x^2} = -\frac{\lambda(1+\lambda)(\lambda-1)}{2G} r^{\lambda-2} \cos(\lambda-2)\theta, \tag{156}$$

$$\frac{\partial^2 u_2}{\partial xy} = -\frac{\lambda(1+\lambda)(\lambda-1)}{2G} r^{\lambda-2} \sin(\lambda-2)\theta, \tag{157}$$

$$\frac{\partial^2 u_2}{\partial y^2} = +\frac{\lambda(1+\lambda)(\lambda-1)}{2G} r^{\lambda-2} \cos(\lambda-2)\theta \tag{158}$$

which satisfies equation(142) if body force vector $\{f\} = 0$. The problem is solved for various sizes of the overlapping domain. The stopping criteria is chosen as 30 iterations or the solution of accuracy 10^{-7}, whichever comes first. Fig. 35 and Table 17 show that more number of iterations are required for smaller overlapping regions. If the overlapping size is fixed, then number of iterations required is dependent upon

Table 18: Number of iterations required to get solution of accuracy 10^{-7} for fixed overlapping domain size(0.5) with various values of r_1 and r_2 for elasticity problem containing singularities

Overlap Size	r_1	r_2	Number of iterations
0.5	0.8	0.3	8
0.5	0.9	0.4	9
0.5	1.0	0.5	10
0.5	1.1	0.6	11
0.5	1.2	0.7	12

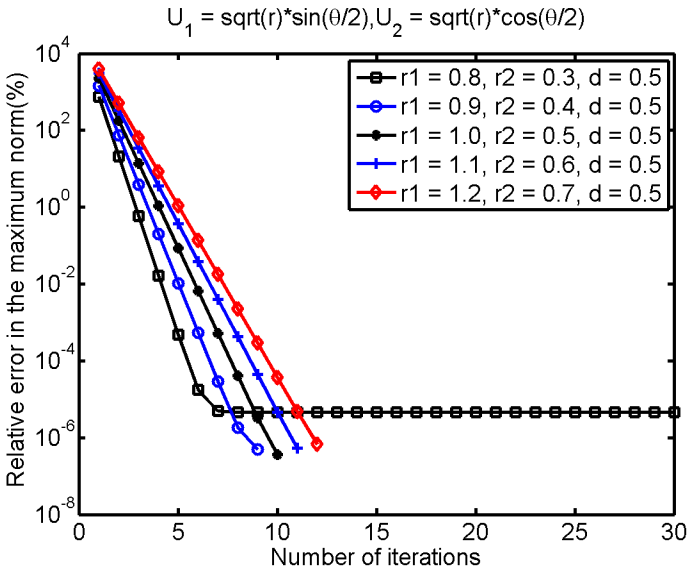

Figure 36: Relative error in the maximum norm in(%) for fixed overlapping domain size with various values of r_1 and r_2 for elasticity problem containing singularities

values of r_1 and r_2. Fig. 36 and Table 18 show relative errors in the maximum norm in percentage for various values of r_1 and r_2. This also shows that if the radius r_2 of the inner circle is very small, then the effect of singularity goes into regular subdomain also and then the solution does not improve after certain number of iterations.

CHAPTER 8: CONCLUDING REMARKS AND ONGOING RESEARCH

In IGA-Collocation method, both modified B-spline basis functions and enrichment by Partition of Unity functions, obtained almost true solutions for problems with regular and singular solutions. In future research work, these methods will be extended to solve elliptic PDEs on non-convex domains like L-shaped, cracked domains and polygonal domains.

Similarly, the Schwarz alternating method in the framework of IGA-Collocation will also be extended to solve elliptic PDEs on non-convex domains. So far this method was applied in elasticity for plane stress and plane strain cases. Future research will test shell and plate problems as well.

Even though the problems that were tested in this dissertation contained only one singularity, we expect that the method can easily be applied to problems with multiple singularities. The Schwarz alternating IGA-Collocation method can be extended to deal with oscillating singularities of the type $r^{\lambda}\cos(\varepsilon \log r), \quad 0 < \lambda, \varepsilon < 1$.

Direct solvers were used to solve problems with the Schwarz alternating method in the frame work of IGA-Collocation. In the future, iterative solvers will also be tested. We will also extend IGA-Collocation approach to the general domain decomposition method.

REFERENCES

[1] Y. Bazilevs, L. Beirao Da Veiga, J.A. Cottrell, T.J.R. Hughes, and G. Sangalli,Isogeometric analysis: Approximation, stability and error estimates for h-refined meshes, Mathematical Models and Methods in Applied Sciences (2006), 1031-1090.

[2] J.A. Cottrell, T.J.R. Hughes, and Y. Bazilevs, Isogeometric analysis: Toward integration of CAD and FEM, 2009.

[3] T.J.R. Hughes, J.A. Cottrell, T.J.R. Hughes, and Y. Bazilevs, Isogeometric analysis: CAD, finite elements, NURBS, exact geometry and mesh refinement, Comput. Methods Appl. Mech. Engrg.(2005), 4135-4195.

[4] H.-S. Oh, J.W. Jeong, and W.T. Hong, The generalized product partition of unity for the meshless methods, J. Comp. Phy. (2010), 1600-1620.

[5] H.-S. Oh, J.W. Jeong, and J. G. Kim, The reproducing singularity particle shape function for problems containing singularities, Comput Mech (2007), 135-157.

[6] H.-S. Oh, J. G. Kim, and W.T. Hong, The piecewise polynomial partition of unity shape functions for the generalized finite element methods, Comput. Methods Appl. Mech. Engrg. (2008), 3702-3711.

[7] H.-S. Oh, J.G. Kim, and J.W. Jeong, The closed form reproducing polynomial particle shape functions for meshfree particle methods, Comput. Methods Appl.Mech. Engrg. (2007), 3435-3461.

[8] D.F. Rogers, An introduction to NURBS, Academic Press, 2001.

[9] Piegl and Tiller, The NURBS book, second edition, Springer, 1995.

[10] H.-S. Oh and I. Babuška, The method of auxiliary mapping for the finite element solutions of plane elasticity problems containing singularities, Journal of Computational Physics (1995), 193-212.

[11] Höllig, K : Finite Element methods with B-Spline, SIAM, 2003.

[12] Han W, Meng X Error analysis of reproducing kernel particle method. Comput. Methods Appl.Mech. Engrg. (2001) 190:6157-6181.

[13] P. Lancaster, K. Salkauskas, Curve and Surface Fitting, An Introduction, Academic Press, San Diego, 1986.

[14] D. Shepard, A two-dimensional function for irregularly spaced data, in: ACM National Conference, 1968, 517-524.

[15] Krishan P.S. Gahalaut, Isogeometric Analysis:Condition Number Estimates and Fast Solvers in:Dissertation, 2013: Johannes Kepler University Linz, Austria.

[16] Hoonjoo Kim, S-J Lee,H.-S. Oh, Numerical Methods for Accurate Finite Element Solutions of Elliptic Boundary Value Problems Containing Singularities, 2002.

[17] P.G. Ciarlet, Basic error estimates for elliptic problems, North-Holland, 1991.

[18] H.-S. Oh and J.W. Jeong, Construction of C^1-basis functions for numerical solutions of the fourth-order partial differential equations, to appear.

[19] Schwarz H.A. úber einen grenzbergang durch alternierendes verfahren. Vierteljahrsschrift der Naturforschenden Gesellschaft in Zurich, 15: pp. 272-286, 1870.

[20] Pierre-Louis Lions. On the Schwarz alternating method. II. In Tony Chan, Roland Glowinski, Jacques Périaux, and Olof Widlund, editors, Domain Decomposition Methods. Second International Symposium on Domain Decomposition Methods, pages 47-70, Philadelphia, PA, 1989. SIAM. Los Angeles, California, January 14-16, 1988.

[21] Alfio Quarteroni and Alberto Valli, Domain Decomposition Methods for Partial Differential Equations book,Editors G. H. Golub, R. Jeltsch, W. A. Light, K. W Morton, E. Sùli, Oxford, 1999.

[22] A. Toselli and O. Widlund, Domain Decomposition Methods- Algorithms and Theory, pages 21-23, Springer, 2005

[23] Dominik Schillinger, John A. Evans, Alessandro Reali, Michael A. Scott, Thomas J.R. Hughes, Isogeometric Collocation: Cost Comparison with Galerkin Methods and Extension to Adaptive Hierarchical NURBS Discretizations.ICES REPORT 13-03, Februray 2013.

[24] S. P. Timoshenko and J. N. Goodier, Theory of elasticity, third edition, McGraw-Hill, Inc, 1970.

[25] F. Auricchio, L. Beirão da Veiga, T.J.R. Hughes, A. Reali and G. Sangalli. Isogeometric collocation methods. Mathematical Models and Methods in Applied Sciences, Vol. 20, No. 11 (2010) 2075-2107

[26] F. Auricchio, L. Beirão da Veiga, T.J.R. Hughes, A. Reali and G. Sangalli. Isogeometric collocation for elastostatics and explicit dynamics. Computer Methods in Applied Mechanics and Engineering, 2012

[27] L. Beirão da Veiga, D. Cho, L.F. Pavarino, S. Scacchi, Overlapping Schwarz preconditioners for isogeometric collocation methods. Computational methods in applied mechanical engineering. 278(2014) 239-253